

Portland State University

**PDXScholar**

---

Dissertations and Theses

Dissertations and Theses

---

1993

# Nucleation and Heat Transfer in Liquid Nitrogen

Eric Roth

*Portland State University*

Follow this and additional works at: [https://pdxscholar.library.pdx.edu/open\\_access\\_etds](https://pdxscholar.library.pdx.edu/open_access_etds)

**Let us know how access to this document benefits you.**

---

## Recommended Citation

Roth, Eric, "Nucleation and Heat Transfer in Liquid Nitrogen" (1993). *Dissertations and Theses*. Paper 1370.

<https://doi.org/10.15760/etd.1369>

This Dissertation is brought to you for free and open access. It has been accepted for inclusion in Dissertations and Theses by an authorized administrator of PDXScholar. Please contact us if we can make this document more accessible: [pdxscholar@pdx.edu](mailto:pdxscholar@pdx.edu).

NUCLEATION AND HEAT TRANSFER IN LIQUID NITROGEN

by

ERIC ROTH

A dissertation submitted in partial fulfillment of the  
requirements for the degree of

DOCTOR OF PHILOSOPHY  
in  
ENVIRONMENTAL SCIENCES AND RESOURCES/  
PHYSICS

Portland State University  
1993

TO THE OFFICE OF GRADUATE STUDIES:

The members of the Committee approve the dissertation of  
Eric Roth presented February 24, 1993.

[Redacted Signature]

Erik Bedegom, Chair

[Redacted Signature]

Jack S. Semura

[Redacted Signature]

Laird C. Brodie

[Redacted Signature]

David H. Peyton

[Redacted Signature]

Randy D. Zelick

[Redacted Signature]

Sergé Prishpionok

APPROVED:

[Redacted Signature]

Robert O. Tinnin, Dean, College of Liberal Arts and Sciences

[Redacted Signature]

Roy W. Koch, Vice Provost for Graduate Studies  
and Research

AN ABSTRACT OF THE DISSERTATION OF Eric Roth for the  
Doctor of Philosophy in Environmental Sciences and  
Resources/Physics presented February 24, 1993.

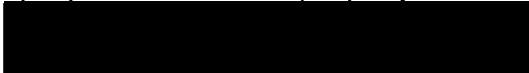
Title: Nucleation and Heat Transfer in Liquid Nitrogen.

APPROVED BY THE MEMBERS OF THE DISSERTATION COMMITTEE:

  
Erik Bodegom, Chair

  
Laird C. Brodie

  
Jack S. Semura

  
David H. Peyton

  
Randy D. Zelick

  
Sergé Prishpionok

With the advent of the new high Tc superconductors as  
well as the increasing use of cryo-cooled conventional  
electronics, liquid nitrogen will be one of the preferred

cryogenics used to cool these materials. Consequently, a more thorough understanding of the heat transfer characteristics of liquid nitrogen is required. In these investigations the transient heating characteristics of liquid nitrogen to states of nucleate and film boiling under different liquid flow conditions are examined. Using a metal hot wire/plate technique, it is verified that there is a premature transition to film boiling in the transient case at power levels as much as 30 percent lower than under steady state nucleate boiling conditions. It is also shown that the premature transition can be reduced or eliminated depending on the flow velocity.

The second part of this research analyses the nucleation (boiling) process from a dynamical systems point of view. By observing how the boiling system variables evolve and fluctuate over time, it is hoped that physical insight and predictive information can be gained. One goal is to discover some indicator or signature in the data that anticipates the transition from nucleate boiling to film boiling. Some of the important variables that make up the boiling system are the temperature of the heater and the heat flux through the heater surface into the liquid nitrogen. Results, gained by plotting the system's trajectory in the heat flux-temperature plane, is that on average the system follows a counterclockwise trajectory. A physical model is constructed that explains this behavior. Also, as the applied heater power approaches levels at which the transition to film is known to occur, the

area per unit time swept out in the heat flux-temperature plane is seen to reach a maximum. This could be of practical interest as the threshold to film boiling can be anticipated and possibly prevented.

## ACKNOWLEDGEMENTS

The culmination and success of this work is largely due to the efforts of people other than myself. At this time I would like to thank those that have had a large influence on my indoctrination and socialization as physical scientist. First, I would like to thank my advisor, Dr. Erik Bodegom for his help in all facets of my education in the laboratory. His patience with the lab neophyte who scarcely knew the difference between an op-amp and an oscilloscope was appreciated. Also, his knowledge of both experimental and theoretical concerns provided a broad base for me to draw on and gave me a wider scientific perspective. More importantly though, through our similar perspectives and shared sense of humor, I hope we remain friends long after my stint at PSU.

As the veteran experimentalists in the lab, Dr. Laird Brodie's insight and skepticism into the techniques and results of my work kept me thinking and honest.

As our labs "resident theoretician" Dr. Jack Semura provided enthusiasm, new ideas and perspectives on projects. It would be fair to say he introduced "chaos" to our lab!

I would also like to thank the Science Support Shop for building and repairing many of the apparatuses used in the experiments. Specifically, Brian McLoughlin and Lee Thanum

for help and instruction in the electronics (Brian must have replaced at least one transistor for each device that I even thought of turning on) and Rudi Zupan and Garo Arakelyan for their skills in machining and constructing the mechanical devices.

I would also like to thank my parents who, though no fault of their own, raised a scientist. They enthusiastically supported all facets of my education, (though they began to wonder why it took me over 25 years to become educated. Maybe it was too many Grateful Dead concerts?)

Lastly, I would like to thank my wife Kirsten for supporting my plans to attend graduate school and putting up with my protracted education until I could finally obtain a "real" job. Though she still isn't quite sure just what it is I do everyday, at least now I will get paid to do it.

## TABLE OF CONTENTS

	PAGE
ACKNOWLEDGEMENTS . . . . .	iii
LIST OF TABLES . . . . .	vii
LIST OF FIGURES . . . . .	viii
CHAPTER	
I INTRODUCTION . . . . .	1
II BASIC HEAT TRANSFER CHARACTERISTICS . . . . .	8
III EXPERIMENTAL PROCEDURE . . . . .	13
Dewars . . . . .	13
Heaters/Thermometers . . . . .	14
Electronics . . . . .	19
Flow Apparatus . . . . .	21
IV RESULTS AND DISCUSSION . . . . .	23
Platinum Wire Results . . . . .	24
Stainless Steel Ribbon Results . . . . .	34
Dewar Geometry . . . . .	41
Summary . . . . .	45
V INTRODUCTION TO NONLINEAR DYNAMICS . . . . .	47
VI REVIEW OF RELEVANT DYNAMICAL CONCEPTS . . . . .	53
VII IMPLEMENTATION OF CONCEPTS IN AN EXPERIMENTAL SITUATION . . . . .	64

VIII DYNAMICAL SYSTEMS RESULTS . . . . .	72
Fourier Transform Results . . . . .	73
Phase Space Reconstructions . . . . .	76
Fluctuations in the $\dot{Q}$ -T plane. . . . .	79
Summary. . . . .	86
IX CONCLUSIONS . . . . .	89
REFERENCES . . . . .	92
APPENDIX . . . . .	96

## LIST OF TABLES

TABLE		PAGE
I	Power Levels for Various Configurations (in $\text{W}/\text{cm}^2$ ) . . . . .	38
II	Peak Heat Fluxes as a Function of Dewar Geometry (in $\text{W}/\text{cm}^2$ ) . . . . .	44

## LIST OF FIGURES

FIGURE		PAGE
1.	Equipment Schematic . . . . .	15
2.	Superheat Temperature $\Delta T$ vs. Time without Forced Convection . . . . .	26
3.	Superheat Temperature $\Delta T$ vs. Time without Forced Convection . . . . .	.28
4.	Superheat Temperature $\Delta T$ vs. Time with Forced Convection . . . . .	.31
5.	Heat Flux $\dot{Q}$ vs. Time without Forced Convection . . . . .	32
6.	Heat Flux $\dot{Q}$ vs. Time with Forced Convection . . . . .	.33
7.	Superheat Temperature $\Delta T$ vs. Time without Forced Convection . . . . .	35
8.	Superheat Temperature $\Delta T$ vs. Time with Forced Convection . . . . .	.37
9.	$\frac{p_v^{tr}}{p_{crit}^{ss}}$ vs. Wire Velocity $v$ . . . . .	43
10.	Dimension as a Scaling Parameter. . . . .	59
11.	Hénon Attractor . . . . .	61
12.	Ln of Correlation Length vs. Ln of Box size for the Henon attractor . . . . .	63
13.	Phase Space Reconstruction of a Time Series by the Method of Delays . . . . .	68

## FIGURE

## PAGE

14.	Amplitude of the Fast Fourier Transform of the Temperature Fluctuations . . . . .	.74
15.	Amplitude of the Fast Fourier Transform of the Heat Flux Fluctuations . . . . .	.75
16.	Ln of Correlation Length vs. Ln of Box size for the Temperature Fluctuation data. . . . .	.77
17.	Fluctuations about the Steady State in the Heat Flux - Temperature Plane . . . . .	.81
18.	Life Cycle of a Bubble in the Heat Flux - Temperature Plane . . . . .	.83
19.	Area per Unit Time Swept Out in the Heat Flux - Temperature Plane . . . . .	.87
20.	Schematic of bubble generator . . . . .	.98
21.	Time Between Bubble Departures vs. Bubble Number . . . . .	101

## CHAPTER I

### INTRODUCTION

Heat transfer is ubiquitous in both nature and any industrialized society. In the environment, the radiant energy of the sun is what drives the weather patterns and consequently the evolving ecosystems. In industry, almost all processes involve the generation of heat, whether it be intentional as part of the manufacturing process or merely as a byproduct required by the second law of thermodynamics. Indeed, many of the limitations of technological or industrial applications are due to the generation of heat coupled with a lack of means to dissipate it effectively. This can strain the efficiency of many processes and consequently underutilize precious human and natural resources. I have decided to study boiling heat transfer in liquid nitrogen.

At first glance, it appears that liquid nitrogen does not have much relation to the environment or availability of resources. But liquid nitrogen's relationship is more subtle in that it will facilitate enabling technologies which will have a direct relationship to environmental concerns. A similar but much more striking analogy is the computer. By itself it is just some electronic wizardry,

but now in the hands of researchers it is used to model, optimize, and understand processes that are of environmental concern. Stated below are some of the reasons that liquid nitrogen is increasingly important.

With the discovery of the new high critical temperature (high  $T_c$ ) superconductors, as well as the increasing use of cryo-cooled conventional electronics, the use of liquid nitrogen as a coolant will expand significantly. The reasons for this are as follows. The new ceramic superconductors have their superconducting transition temperature near 120 K, and for these superconductors to have electrical characteristics that are stable with respect to temperature variations they need to be cooled to values approximately two thirds of the transition temperature. Therefore a cooling liquid that has its boiling point at two thirds of this temperature is necessary [1]. Liquid nitrogen (LN<sub>2</sub>) has a boiling point at one atmosphere of 77 K so it satisfies that requirement.

It has been found that many conventional semiconductor devices have enhanced electrical performance when cooled to cryogenic temperatures. Such enhancements include faster switching speeds, lower noise levels and power dissipation, and greater reliability [2]. Also, there are a number of reasons besides the low normal boiling point that LN<sub>2</sub> is the preferred cryogen for both technologies. First, LN<sub>2</sub> is a good dielectric and thus prevents any undesirable electrical

interactions with the electronic apparatus being cooled [3]. Second, LN2 is relatively inert, so that there is little chance that the LN2 will degrade the devices that it cools. Third, compared to other cryogenics, LN2 is a renewable resource, therefore a virtually unlimited supply of nitrogen exists. Also, LN2 is generally the least expensive and one of the most widely used cryogenics in industry.

Therefore, assuming LN2 as the optimal cryogenic coolant for the majority of electronics applications, a qualitative as well as quantitative knowledge of its heat transfer characteristics is required.

In general, systems that involve cryogenic fluids have not been studied as much as the conventional coolants like water. One reason is that it has been only in the past few decades that cryogenic technology has been incorporated into industrial applications on a large scale. Though there is no fundamental physical difference between cryogenic and noncryogenic fluids (excepting superfluid helium), the experiments that one must do are more difficult to perform because of the necessary cryogenic environment [4]. Finally, a theoretical analysis of solids or fluids at cryogenic temperatures is more difficult to perform because of the often strong temperature dependence of their physical properties such as the heat capacity and the thermal conductivity [5].

The system chosen for this investigation involves heat

transfer from a solid into the cryogen liquid nitrogen, under steady state as well as transient conditions. The primary mode of heat transfer investigated is boiling, as this is the dominant mode for the heat fluxes anticipated in applications. Properties studied include the peak steady state nucleate boiling heat flux and the maximum temperature to which the liquid can be superheated before boiling occurs. Nucleate boiling is the process of evaporation associated with vapor bubbles in liquid. Superheating is the process of raising the temperature of the liquid above its normal boiling point. A superheated liquid is a thermodynamically metastable state. It has been shown that these values can vary depending on the way in which heat is applied to the liquids. Specifically, for abrupt step increases of applied power, the maximum allowed power before film boiling occurs can be as little as 40% of the maximum peak steady state nucleate boiling heat flux [6]. (Film boiling is a form of boiling heat transfer in which an insulating vapor film is formed between the heater surface and the liquid.) This effect is called a "premature" transition to film boiling. This premature transition to film boiling could be an important consideration in the design of heat transfer systems. For example, transient heating may induce film boiling thus preventing efficient cooling of the device and result in burnout of expensive or critical components of a system. Previous work by Sinha et

al indicates that the reason for its occurrence is the lack of a well developed natural convection current [6]. The driving force for natural convection is the heat input itself. In transient heating this convection current does not have time to build up to its steady state value, hence the premature transition. However, the study of Sinha et al did not give useful quantitative data. In this study, such data are generated by creating forced LN2 convection. The results show that in some cases, with flow velocities up to 50 cm/s, the premature transition can be suppressed for power levels approaching that of the steady state peak nucleate boiling heat flux [7]. It should be pointed out that this premature transition to film boiling was not observed by Giarratano [8], but several differences between the experimental conditions of Giarratano and Sinha exist. The differences are in the ambient pressure and temperature, the wire diameter, and the heat leak into the dewar.

In this research I intend to clarify and define the limits within which liquid nitrogen can be used as a coolant for heat generating devices. This dissertation is divided into two parts. The first part deals with measurements of temperature and heat flux under conditions of steady state and transient heating. The second part is an analysis of the steady state measurements from a dynamical systems point of view to see whether any predictive information can be gained.

In this first part I use a standard approach to heat transfer problems. A thin wire or a flat plate immersed in a bath of liquid nitrogen is heated and the temperature as a function of time is recorded. By also recording the applied heater power, the heat flux into the liquid is calculated as a function of time. The maximum values of these quantities that occur are of primary concern, as one is often interested in the question: "How much heat must be dissipated before the device fails to work properly or self-destructs?" The maximum temperature and heat flux attained have different importance for conductors, superconductors, and semiconductors.

For example, one does not expect superconductors to generate any heat as they have no D.C. electrical resistance. However, in a type 2 superconductor magnetic flux lines (fluxoids) penetrate into the superconductor and, as a result of their unpredictable motion, generate heat. At the point or region where the fluxoid moves there will be some small amount of heat generated. Under A.C. current conditions the phenomenon is aggravated and the conductivity becomes finite [9]. Another source of heat generation is due to the extreme mechanical stresses that can occur in a superconducting magnet assembly. There, the forces induce movement of the coil wires and frictional heating results. The critical factor in all the above circumstances is that the heat be conducted away before it causes a local

temperature rise of the superconductor above its transition temperature. Otherwise, the resistive portion of the material could grow and the resultant Joule heating could destroy the device.

For conventional semiconductor chips the average power generated can be quite high. In fact, one of the limiting factors in preventing higher chip densities or higher clock speeds is the problem of heat dissipation, since insufficient heat removal is highly correlated with premature failure [3].

Experiments in this dissertation were designed in view of the different requirements of these superconductor and semiconductor systems. Heat transfer characteristics from a solid to LN2 are studied under various conditions. The specific conditions varied were:

- 1) steady state and transient heating power;
- 2) forced flow of the liquid or a stationary bath;
- 3) different dewar geometries;
- 4) geometries and materials for the heater.

My results indicated that all the above conditions have a significant effect. The lack of carefully specifying the above conditions may be the reason for the large range of values for the maximum nucleate boiling heat flux of liquid nitrogen that have been reported in the literature [10].

## CHAPTER II

### BASIC HEAT TRANSFER CHARACTERISTICS

In this Chapter I describe some of the relevant concepts, vocabulary and mechanisms involved in the study of heat transfer. Heat transfer is known to occur in several modes. These different modes are conduction, convection, radiation, and boiling [11]. Conduction heat transfer is due to the interatomic interaction of molecules i.e., sharing of energy through collisions when a temperature gradient exists in the medium. This can occur in any phase or type of material. Convection is a form of heat transfer that can only occur in a fluid (gas or liquid) in a gravitational field. This occurs when a temperature gradient causes the density of the fluid to vary in different parts of the fluid. This variation in fluid density in conjunction with gravity, is the driving force for the mixing of the fluid. Heat transfer is thus enhanced over pure conduction conditions. Radiation heat transfer exchanges energy through the electromagnetic field. However, for this study and the small superheat conditions under which it was done, radiation heat transfer can be neglected.

Boiling is different from the above three mechanisms in

that the energy transfer primarily occurs through the latent heat of vaporization of the liquid. That is, energy is removed from the hot surface when a vapor bubble is formed from the liquid and then is transported to a cooler environment where it either collapses back into the fluid or is vented to the outside atmosphere. Also, due to the agitation produced by the bubble motion through the liquid there is some boiling induced convection that occurs. Each of these modes is dominant under different conditions, which are determined by temperature, temperature gradient, ambient pressure, and type of liquids involved, and so forth [4]. Boiling is generally the most efficient form of heat transfer in cryogenic fluids. In this study, the stress is on conduction, convection, and in particular boiling.

Boiling can be divided into two different categories, nucleate and film boiling [11]. Nucleate boiling from a solid surface is commonly what one observes in water. Bubbles form at particular nucleation sites on the heated material. The bubbles grow in size and then detach from the surface when the buoyant forces overcome the cohesive forces of surface tension. Typically these sites are microscopic cracks and crevices in the material that contain "seeds" of vapor. Nucleate boiling is also called heterogeneous nucleation because the bubble forms at the interface between two different substances (e.g., the liquid nitrogen and the solid heater material) [12].

Film boiling can be considered an extreme case of nucleate boiling. That is, for increasing heat fluxes, the bubble formation on the surface of the material occurs so rapidly that the bubbles do not have time to detach and be replaced by liquid. The result is that nearby bubbles coalesce and a vapor film covers the surface and impedes further heat transfer due to the insulating effect of the vapor film. This in turn drives up the temperature difference between the heat producing object and the surrounding liquid. The heat flux at which this occurs is termed the critical heat flux. In liquid nitrogen the increase in temperature due to film boiling can approach hundreds of degrees over that of nucleate boiling for the same heat flux. Such a large temperature increase is usually detrimental to the heat producing device and thus should be prevented. The critical (or peak) heat flux is the maximum attainable heat flux just before the transition from nucleate boiling to film boiling occurs. This heat flux is achieved by slowly increasing the heater power until film boiling occurs [13].

Contrasted to heterogeneous nucleation is homogeneous nucleation in which the vapor "seed" originates in the bulk of the fluid and not at the interface between liquid and solid [14]. It is known that a liquid can withstand a certain amount of superheat (i.e., heated above its normal boiling point) in the absence of external initiating

influences, before a transition to the vapor phase takes place. In a pure liquid such as nitrogen, this superheat approaches several tens of degrees [15]. The transition occurs when a sufficiently large number of vapor nuclei, induced by thermodynamic fluctuations in the liquid, reach a critical radius and grow spontaneously in the liquid. This causes the very rapid formation of many bubbles in the superheated liquid adjacent to the wire. The spontaneous initiation of homogeneous nucleation and the subsequent cooling effect restricts further increases in the temperature. Although the temperature at which this occurs is not defined precisely, the kinetic theory of homogeneous nucleation predicts the nucleation rate to depend exponentially on parameters related to the degree of superheat [14]. Thus in practice a relatively sharp superheat maximum is attained. For LN<sub>2</sub> this temperature is 110 K at 1 atmosphere.

It also appears that how the heat flux is applied can have an effect on the critical heat flux. Some authors have found that for sudden step increases of power application the maximum allowed heat flux before film boiling occurs can be as little as 40% of the critical heat flux [6]. This effect is called a premature transition to film boiling.

Note that under slightly different experimental conditions, this phenomena was apparently not observed by other investigators [8]. Thus, there still is a question as

to the existence of this phenomenon and under which specific conditions it occurs.

In this study I investigated nucleate boiling and the conditions under which the transition to film boiling occurs in liquid nitrogen. I thus sought to clarify the occurrence of the premature transition to film boiling and investigate methods to reduce, eliminate, and/or predict the transition to film boiling.

## CHAPTER III

### EXPERIMENTAL PROCEDURE

A brief synopsis of the experimental setup is given here. More detailed subsections follow. The experiments were conducted in dewars of varying sizes and geometry. Also, heaters and thermometers of different materials and geometry were tried. Measurements of the voltage and current signals were made to determine temperature and applied heater power. Forced convection was achieved by moving the heater through the stationary liquid in the dewar. Finally, a computer was used to automate the experiments and digitize the data for later retrieval and analysis.

### DEWARS

The experiments were conducted in cylindrical dewars vented to atmospheric pressure. The capacity of these dewars varied from 1 to 35 liters. The diameter and length respectively for these dewars were 7 by 30 cm (glass), 5 by 50 cm (glass), and 35 by 40 cm (steel). One configuration had the smaller of the glass dewars inserted into the larger one so that better insulation could be achieved. Because of the variability of insulation in the dewars, heat leak into

the containers caused the bath of nitrogen to vary from a very quiescent state as in the in the steel storage dewar to one of steady boiling which occurred for the smaller glass dewar.

#### HEATERS/THERMOMETERS

Three different geometries for the heater/thermometer were used. The first heater/thermometer assembly used was composed of a 8 cm length of platinum wire 0.1 mm in diameter (See Figure 1). To minimize the effect of heat loss by conduction through the two voltage leads, fine wires were used as the voltage sensing leads, and were soldered 1.5 cm from each end of the wire. Thus the effective thermometer length was 5 cm [16]. The other two heater/thermometer assemblies used were composed of a 6 cm length of "302" stainless steel ribbon 0.05 mm thick and 0.2 and 1.0 cm width. Similar precautions to prevent heat leak through the voltage and current leads were taken. These geometries were chosen because they are similar to those which are found in electronics applications utilizing wires and integrated circuits. The heater surfaces were oriented vertically in the dewar. The two primary measurements made were the temperature and the heat flux into the liquid, both time dependent quantities.

The method of heat generation and temperature measurement was accomplished by the same instrument and is

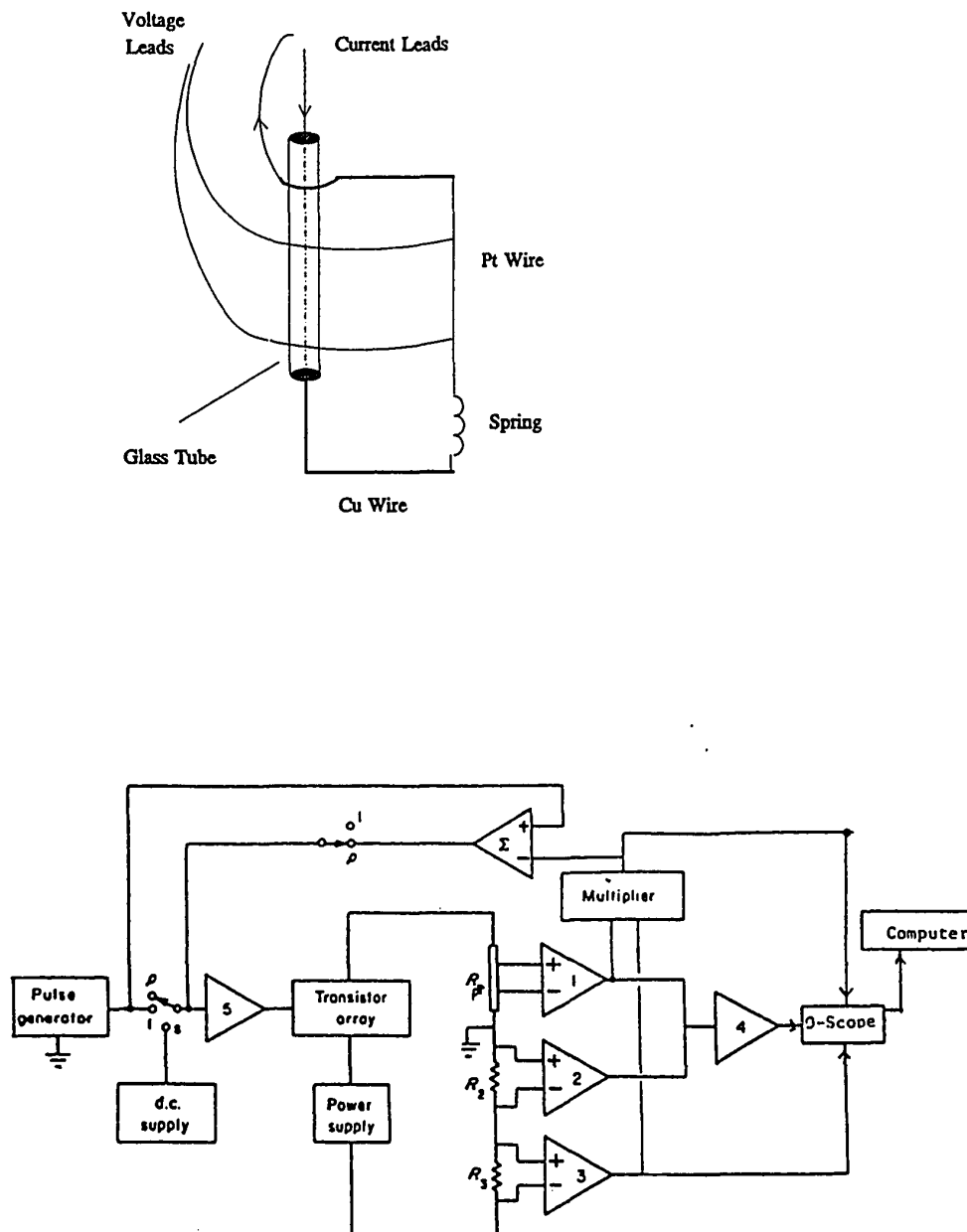


**Figure 1.** Equipment schematic. Upper diagram is platinum heater thermometer. Lower diagram is circuit schematic for experimental control and data acquisition.

known as hot wire thermometry [17]. The basis for this technique is essentially resistance thermometry, with the additional function that the material used to measure the temperature is also the one that generates the heat flux into the medium. This alleviates the problem of imprecise determinations of the temperature and heat flux when the heater and thermometer are spatially separated. The heating current (a few amperes in the case of the platinum and tens of amperes for the steel) was controlled by an op-amp/transistor array described in the next section.

The temperature change of the heater as a function of time was determined by measuring the resulting change in electrical resistance of the heater since the electrical resistance is a well characterized property of a metal. In particular, the electrical resistance is a monotonically increasing function of the temperature that typically has a linear dependence on the temperature over a narrow temperature range. However, some metals are more strongly temperature dependent (i.e., they possess a larger temperature coefficient) than others, and some are closer to linear in their temperature dependence than others. These properties determine the sensitivity with which the temperature can be measured and the ease in calibrating such a device. The metals used were platinum and stainless steel, of which the former has the most linear and largest temperature coefficient of the metals. At 77 K platinum's

resistivity changes 2% per degree. Both metals have temperature coefficients that are very stable over time and it do not react readily with other substances. The temperature coefficient of both platinum and stainless steel were very close to linear in the temperature range of interest, so the calibration method was to record resistance measurements at the two temperature extremes and interpolate. The two end points chosen were the saturated bath temperature  $T_b$ , (77.3 K @ 1 atmosphere pressure) and room temperature (293 K). The temperature coefficients calculated were checked against handbook values and found to agree within 5 percent [18]. To calculate the temperature, a known current was passed through the material. Simultaneously, measurements of the voltage difference between two points of the "resistor" were made. From these measurements one calculated the resistance using Ohm's law, and thus the temperature.

Another consideration is that the measurements of the temperature and heat flux are transient, so that the thermometer had to be able to track rapid temperature changes. That is, the heater thermometer had to be in thermal equilibrium with the liquid immediately surrounding it at times scales on the order of a millisecond. This time scale was determined by observation of nucleate and film boiling processes at the heat flux levels of interest in this study. The thermal response time is a function of the

material and its geometry, and was calculated by the following equation.

$$\tau = d^2 / \kappa \quad (1)$$

where

$$\kappa = k / \rho c \quad (2)$$

and  $d$  is a characteristic dimension of the material, such as the thickness of the wire or the ribbon.  $\kappa$  is the thermal diffusivity,  $k$  is the thermal conductivity,  $\rho$  is the density, and  $c$  is the specific heat. For the platinum wire and the stainless steel ribbon the time constants were 60  $\mu$ s and 500  $\mu$ s respectively. Note that these thermophysical properties changed with temperature, but that in the temperature changes encountered (20 degrees celsius), this amounted to less than a 15% change in the time constant.

The overall uncertainty in determining the heater temperature had two contributions. First, was determining the superheat temperature, that is the temperature changes relative to the ambient bath temperature. This uncertainty was effectively a function of the precision with which the current, voltages, resistance, temperature coefficient, and amplifier gains could be determined. This uncertainty was estimated to be no more than 0.3 degrees celsius over a 20 degree temperature span. There was an additional uncertainty due to the precision that the saturation bath

pressure was known and the ability to electronically subtract out the corresponding ambient bath temperature value from the signal. This was estimated to be 0.3 degrees celsius as well. However, the sensitivity, which was determined by the effective length of the heater/thermometer and the noise in the electronics and environment, was of the order of millikelvins.

The limiting factors in determining the overall accuracy in heat flux were the precision of the current, resistance, and the geometric measurements for the material. The accuracy for the heat flux was found to be 5%.

#### ELECTRONICS

The circuit schematic for the metal heater/thermometer and the associated electronics is shown in Figure 1 and described below. The output of a pulse generator or a D.C. voltage source, was sent to a current amplifier which was configured to supply a constant current to the heater/thermometer. In series with this were two 100 watt, 0.25 ohm resistors. These resistors had a low temperature coefficient so as to minimize heating errors when reading large currents. Instrumentation amplifiers 1 and 3 amplified the voltage  $V_{Pt}(t)$  across the platinum wire  $R_{Pt}$ , and the voltage  $V_I$  across resistor  $R_3$  respectively.  $R_{Pt}$  can be thought of as being composed of two contributions, a temperature independent term called  $R_0$ , and the temperature

dependent term called  $\Delta R(T)$ . On an absolute scale the temperature coefficient of metals were small and thus the majority of the measured signal of  $V_{pt}(t)$  was due to the temperature independent part of the resistance  $R_0$ , and was called  $V_0$ . Frequently one is interested in the superheat temperature  $\Delta T(t)$ . The temperature changes about the normal boiling point (i.e. for LN2,  $\Delta T(t) = T(t) - 77.3$  K). Therefore, in order to produce a signal reflecting only the superheat temperature, the constant portion  $V_0$  must be electronically subtracted from  $V_{pt}(t)$  to yield  $\Delta T(t)$ . This was accomplished by manually adjusting the gain from amplifier 2 so that the output of amplifier 4 is zero when no superheating has occurred. This balancing procedure was implemented when the heater/thermometer was known to be at 77.3 K as is the case at the very beginning of the current pulse. The signals from amplifiers 3 and 4 were then recorded on a digital oscilloscope. Then the digitized data were stored in the computer for further manipulation.

The equations to solve for the superheat temperature  $\Delta T(t)$  follow.

$$V_{pt}(t) = V_0 + \Delta V(t) = IR_{pt} = I(R_0 + \Delta R(t)) \quad (3)$$

$$V_{pt}(t) = IR_0(1 + \alpha \Delta T(t)) \quad (4)$$

Solving for  $\Delta T(t)$  gives

$$\Delta T(t) = \frac{\Delta R(t)}{R_0 \alpha} = \frac{(V_{pt}(t) - IR_0) / I}{R_0 \alpha} \quad (5)$$

where  $V_{pt}(t)$  was the voltage difference between two points on the heater/thermometer,  $V_0$  was the voltage due to the temperature independent part of the resistance  $R_0$ .

$V_I$  was the voltage across the 0.25 ohm resistors and was directly proportional to the current  $I$  through the heater/thermometer,  $\alpha$  was the temperature coefficient for the particular metal and  $\Delta T(t)$  was the calculated superheat temperature above 77.3 K.

#### FLOW APPARATUS

In order to enhance heat transfer one common technique is to use forced convection. Forced convection was achieved in this work by moving the heater/thermometer either up or down in the dewar by means of a variable speed DC electric motor. The reason for moving the heater/thermometer rather than generating a flow of liquid nitrogen is that the motor induced flow was easier to measure and control. The apparatus was assembled as follows. An electric motor had a round gear at one end of its drive shaft. This gear meshed with a rigid linear rack (approximately 50 cm long) oriented vertically. The rack was held in place by idler wheels and only allowed to move in the vertical direction. Attached to the bottom of the rack was the heater/thermometer assembly.

Thus there was just under 50 cm of vertical travel. With the particular gear ratios, motor assembly, and dewars utilized, maximum velocities of 50 cm/sec were possible. The velocity was determined by a photogate timer which measured the time which a 1 cm vane attached to the heater/thermometer shaft took to pass through the photogate.

The uncertainty in controlling and determining the velocity was due to two factors one; the ability to regulate the current to the electric motor, and two, the resolution with which the vane geometry and timer measurements could be determined. I measured the variation in these parameters and found the overall uncertainty in velocity is 6 percent.

Both the movement of the heater/thermometer assembly and the heating current through it were controlled and coordinated by a computer. A typical run proceeded as follows. First, the computer sent a signal to initiate the flow. Second, after allowing sufficient time for the flow to stabilize (0.2 sec) the heater/thermometer was pulsed with current (typically for 0.65 sec) and the resulting signals were recorded on the digital oscilloscope. Third, the flow was stopped, and the oscilloscope sent the digitized traces to the computer for storage. The thermometer assembly was backed up to its original position. This sequence was then repeated after 2 minutes to allow the LN<sub>2</sub> to settle down. For each applied power setting and velocity, several runs were taken to insure reproducibility.

## CHAPTER IV

### RESULTS AND DISCUSSION

The only two measurements that were made during a "run" were the voltage across the heater/thermometer and the current through it as a function of time. From these data one could calculate the resistance, and thus temperature of the wire, the total power dissipated in the wire, and the total heat flux out of the wire and into the liquid. This first section describes how the heat flux analysis was performed (the temperature calculation was explained in Chapter III).

The heat flux  $\dot{Q}(t)$ , is not simply the total power dissipated per unit area, as was the case for steady state heat flux experiments. There is a correction term due to the non-zero heat capacity of the wire. This is given by the following equation.

$$P(t) = \dot{Q}(t) + C \frac{dT}{dt} \quad (6)$$

where  $C$  is the heat capacity per unit surface area of the wire and  $P(t)$  is the total applied power per unit surface area of the wire (ie.  $I^2 R(t)/A$ ). The applied power increased with time since the resistance of the wire is increasing with temperature. This was accounted for when

the calculation of  $P(t)$  were made on the computer and plotted. However, references made to different heating curves indicate their initial power dissipation at  $t=0$ . Since the temperature of LN2 is significantly below the Debye temperature of platinum and stainless steel, the heat capacity varied significantly as a function of temperature. This was adjusted accordingly when the calculations are made.  $dT(t)/dt$  is the time rate of change of the temperature of the wire and this was obtained numerically. Thus it is seen from Eqn. 5 that because of the non-zero heat capacity, in the transient case the heat flux into the fluid could be greater than or less than the applied power. In the true steady state case the two are equal.

In addition to the transient measurements mentioned above, measurements were also made to determine the peak steady state heat flux. As a reference, the maximum value of the steady state peak heat flux for the three heaters was  $9.5 \text{ W/cm}^2$ . This was for the platinum wire heater surface. Peak steady state heat flux values lower than this were also obtained and it is shown later that these values depend on the dewar and heater geometry. The figures and discussion were separated on the basis of the heater material.

#### PLATINUM WIRE RESULTS

Figure 2 shows the superheat temperature vs. time under no flow conditions. The figures were labeled in terms of

the initial applied power. This was done to provide a reference since in these constant current experiments the resistance was increasing with temperature and thus the power level increases as well. For an initial applied power of  $2.3 \text{ W/cm}^2$  the temperature rose steadily. At this particular current the onset of nucleate boiling occurred after 600 ms, after which the temperature of the wire drops to 4 kelvins above the bath temperature. At a slightly larger power ( $2.4 \text{ W/cm}^2$ ) a transition to film boiling occurs as could be observed by the abrupt increase in the slope of the temperature-time curve at 450 ms. This transition is called premature because the transition to film boiling occurred at power levels less than the peak steady state nucleate boiling heat flux of  $9.6 \text{ W/cm}^2$ . When the effect of the increased resistance was included in the heat flux calculation, the premature transition to film boiling was seen to occur at nearly 30% of the peak nucleate boiling heat flux. At even higher power levels the transition to film boiling occurred at earlier times and higher superheat temperatures were reached before film boiling commences.

Figure 3 shows the nucleate boiling stage in more detail and from a different data set. For comparison, a heating curve (curve A) is included which shows the theoretical result for a wire with constant power dissipation. It was assumed that only conduction occurs and that there is no temperature gradient in the wire. This

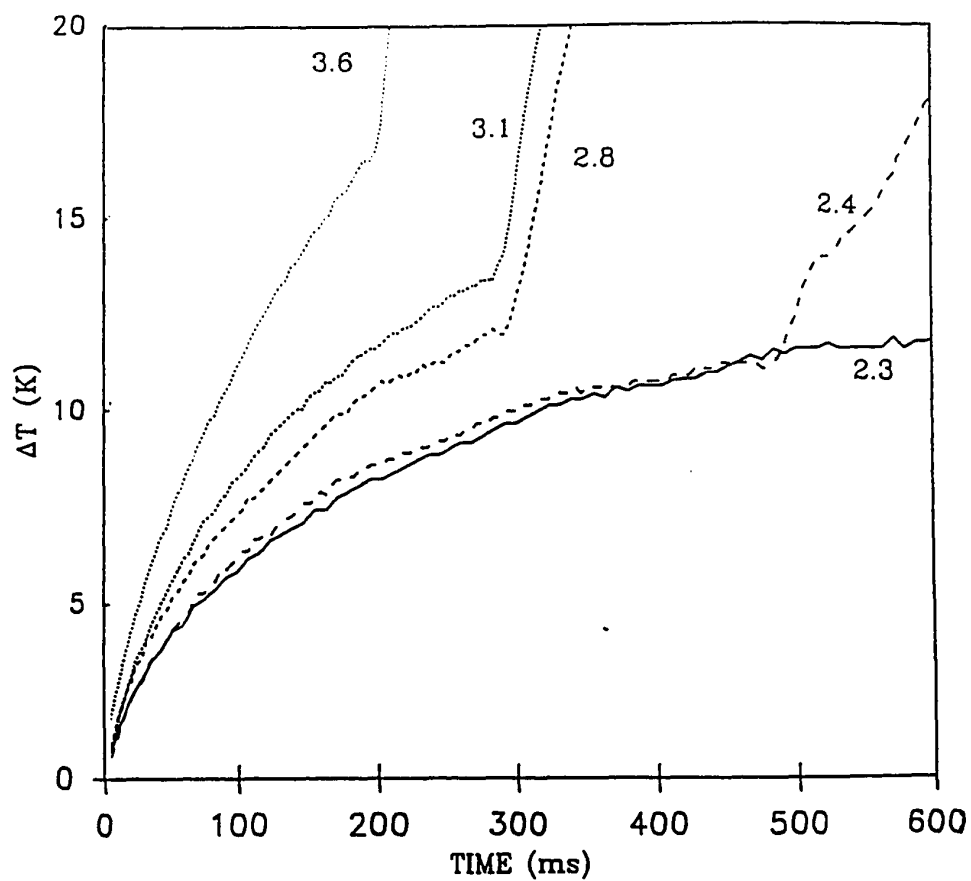


**Figure 2.** Superheat temperature  $\Delta T$  vs. time without forced convection. The temperature response as a function of time is shown for the platinum wire with a step function of current initiated at  $t=0$ . The value adjacent to each curve indicates the initial applied power per unit area in  $\text{W/cm}^2$ .

latter assumption was justified because platinum's thermal conductivity is nearly 600 times greater than LN2. In this case the analytical solution is given by [19]:

$$T(t) = \frac{2q\alpha^2}{\pi^3 K} \int_0^\infty \frac{(1 - e^{-\frac{\kappa t u^2}{a^2}}) u^{-3} du}{[uJ_0(u) - \alpha J_1(u)]^2 + [uY_0(u) - \alpha Y_1(u)]^2} \quad (7)$$

where

$$\alpha = \frac{2\rho_{LN2} C_{LN2}}{\rho_{Pt} C_{Pt}} \quad (8)$$

is a parameter which is twice the ratio of the heat capacity of an equivalent volume of the medium (LN2) to that of the conductor (platinum). It is 1.74 at 80 kelvins.  $K$  is the thermal conductivity of the LN2, and  $q$  is the heat generated per unit length of the wire.  $\kappa$  is the thermal diffusivity for the LN2 defined earlier (Equation 2). The radius of the wire is denoted by  $a$ .  $J_0(u)$  and  $J_1(u)$  are Bessel functions of the first kind, of order zero and one respectively.

$Y_0(u)$  and  $Y_1(u)$  are Bessel functions of the second kind, of order zero and one respectively. For a short time it can be seen that the analytical curve and the experimental curves agree. When the experimental curves begin to diverge from the analytical one, modes of heat transfer other than conduction are commencing.

The three other curves (curves B,C,D) were from experiments under "identical" conditions of an initial applied power of 3.7 W/cm<sup>2</sup> and without forced convection.

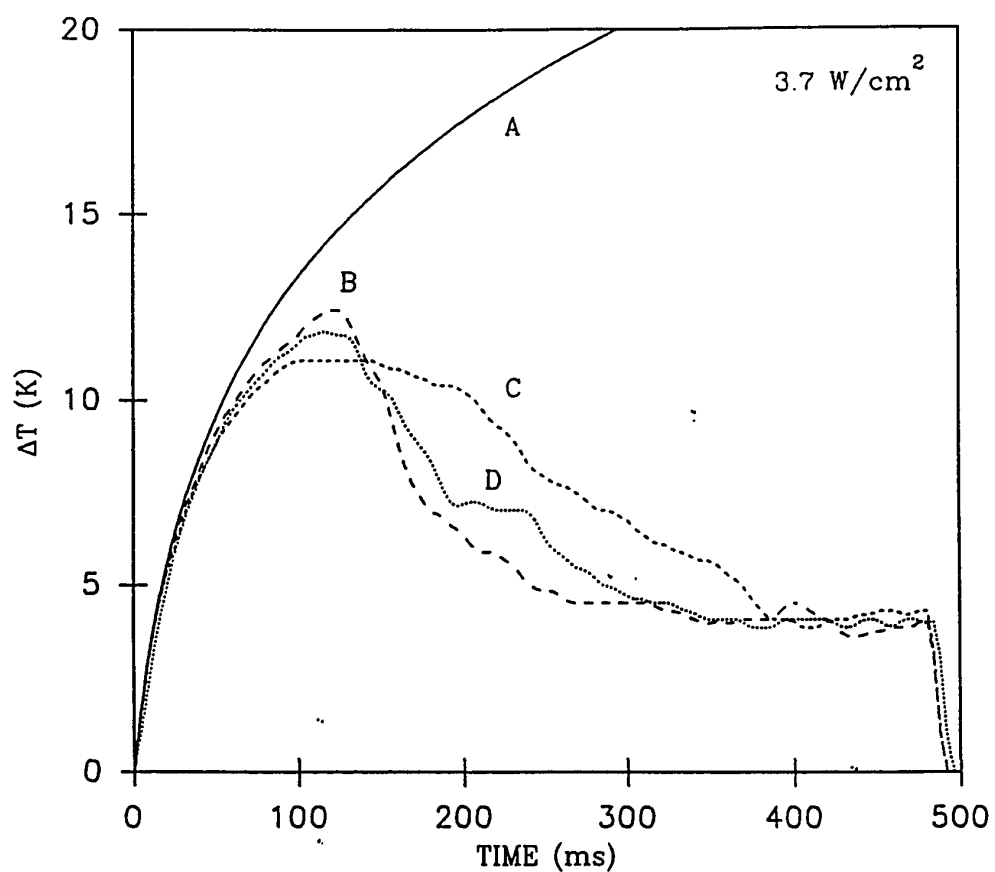


**Figure 3.** Superheat temperature  $\Delta T$  vs. time without forced convection. The temperature response as a function of time is shown for the platinum wire with a step function of current initiated at  $t=0$ . The initial applied power is  $3.7 \text{ W/cm}^2$ .

Curve A began to deviate from the others at approximately 50 milliseconds. The three experimental curves also initially coincide but at 50 milliseconds began to separate. After approximately 100 milliseconds nucleate boiling is well developed as seen by the smooth decrease in temperature. The temperature of the surrounding fluid finally reduces to approximately a 4 degree superheat. The difference between the maximum temperature superheat (12 degrees) and the steady state nucleate boiling superheat (4 degrees) is called "overshoot". The value of this overshoot is an important design criterion for superconductors, as one wants to prevent the critical temperature from being exceeded or wide temperature variations from occurring. Overshoot is due to a lag in the onset of steady state nucleation at the surface of the wire. That is, initially all the nucleation sites are not active. This hysteresis effect is common in the cryogenic fluids because they wet surfaces very well and significant superheats are often required to activate them.

One other feature that stands out in the three experimental curves in Figure 3 is that the curves deviated from one another between 100 and 400 ms. This was typical for data collected under "identical" conditions. The origin of this variation was that the experiment is not done under equilibrium conditions. Because the definition of superheating a liquid is to bring the liquid into a metastable state, the higher the superheat the farther from

equilibrium the system is and thus the system is increasingly unstable. This instability makes the system's evolution extremely sensitive to the initial conditions. For example, a slight difference in the temperature profile, the convection pattern, or even a stray bubble in the liquid might make a difference as to which path the system "chooses".

Figure 4 emphasizes the aforementioned instability of the system and shows that under "identical" conditions of flow and applied power the system either went into nucleate boiling or film boiling. Thus these initial conditions appear to be on the dividing line between the two routes the system can take.

Figures 5 and 6 are from the same data sets as Figures 3 and 4 respectively. However, these show the calculated heat flux  $Q(t)$  vs. time curves as discussed previously. These curves also appear to follow similar paths for a short time and then separate. The abrupt heat flux peaks in Figure 6 indicate that vapor formation is occurring, thus cooling the superheated liquid. As long as the vapor formation does not occur too quickly and extensively film boiling did not occur. It is seen that the two curves that go into film boiling achieved a higher superheat, and consequently were more unstable. Also note in these plots, prior to film boiling, the transient heat flux never exceeded the steady state value. In fact, the transition to

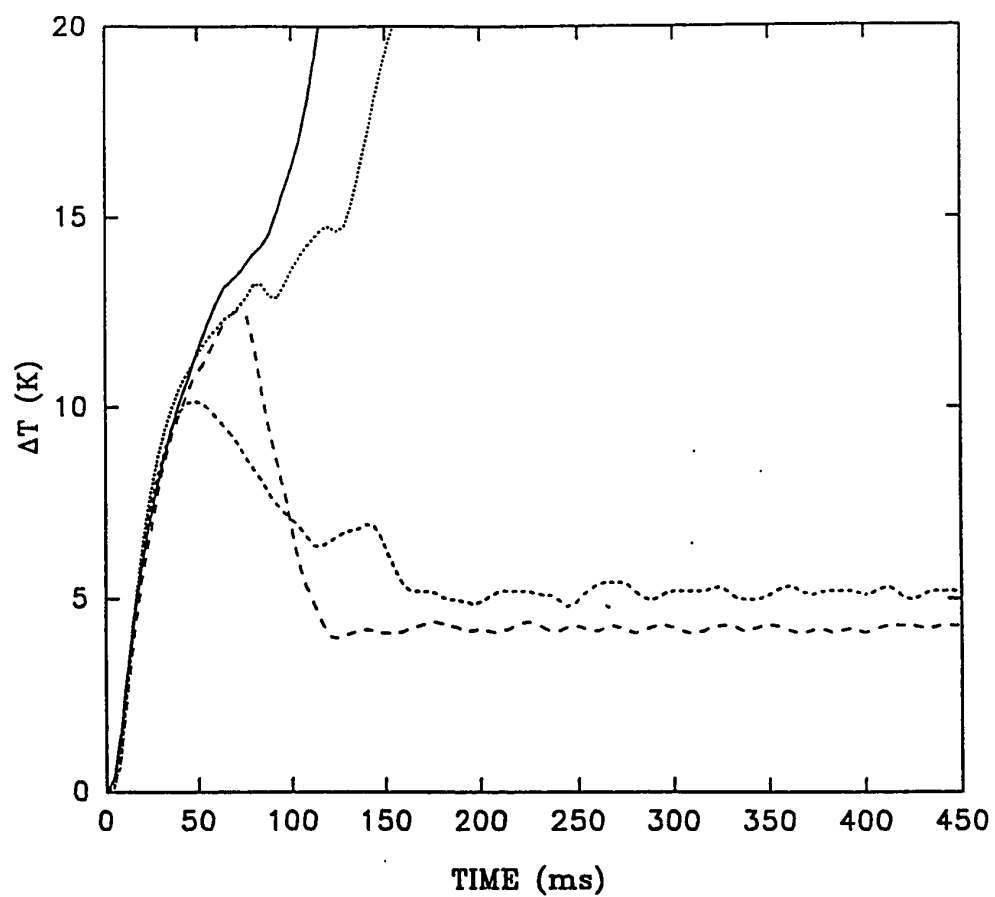


**Figure 4.** Superheat temperature  $\Delta T$  vs. time with forced convection. The temperature response as a function of time is shown for the platinum wire for four "identical" heat pulses and flow rates. The initial applied power is  $5.4 \text{ W/cm}^2$ . The flow rate is  $21.7 \text{ cm/sec}$ .

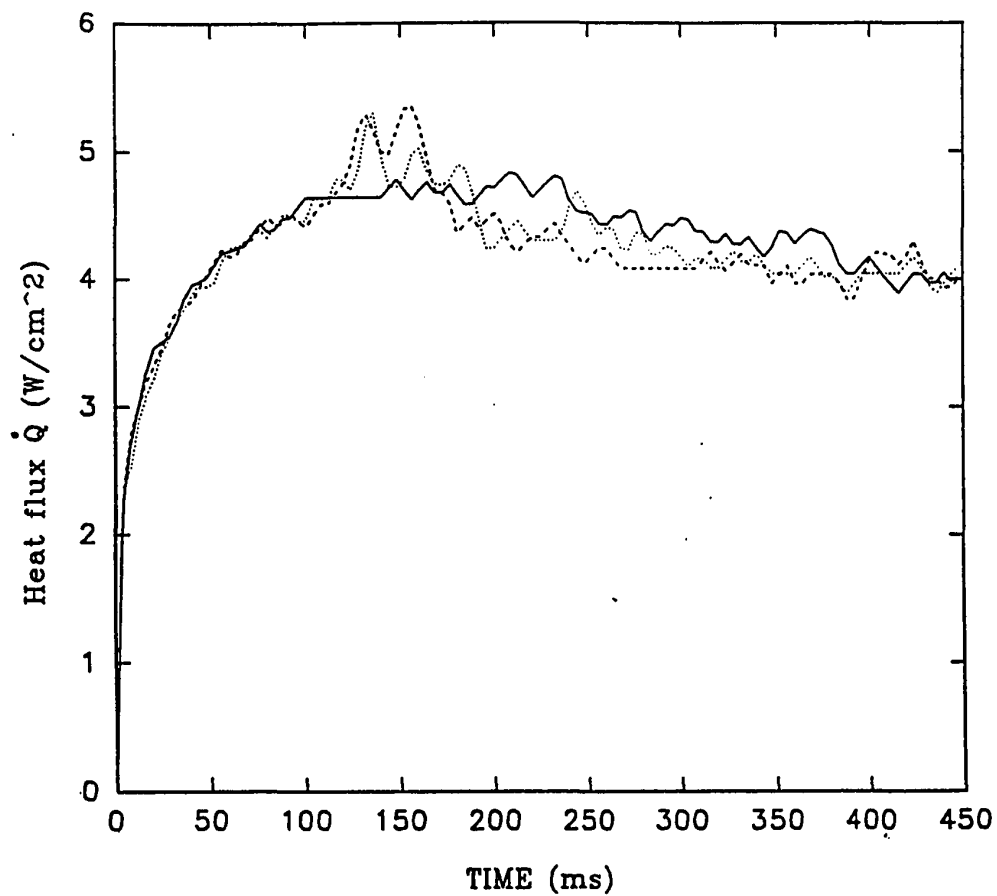


Figure 5. Heat flux  $\dot{Q}$  vs. time without forced convection. The heat flux  $\dot{Q}$  as a function of time is shown for the platinum wire with a step function of current initiated at  $t=0$ . The initial applied power is  $3.7 \text{ W/cm}^2$ . Plot was derived from same data set as Figure 3.

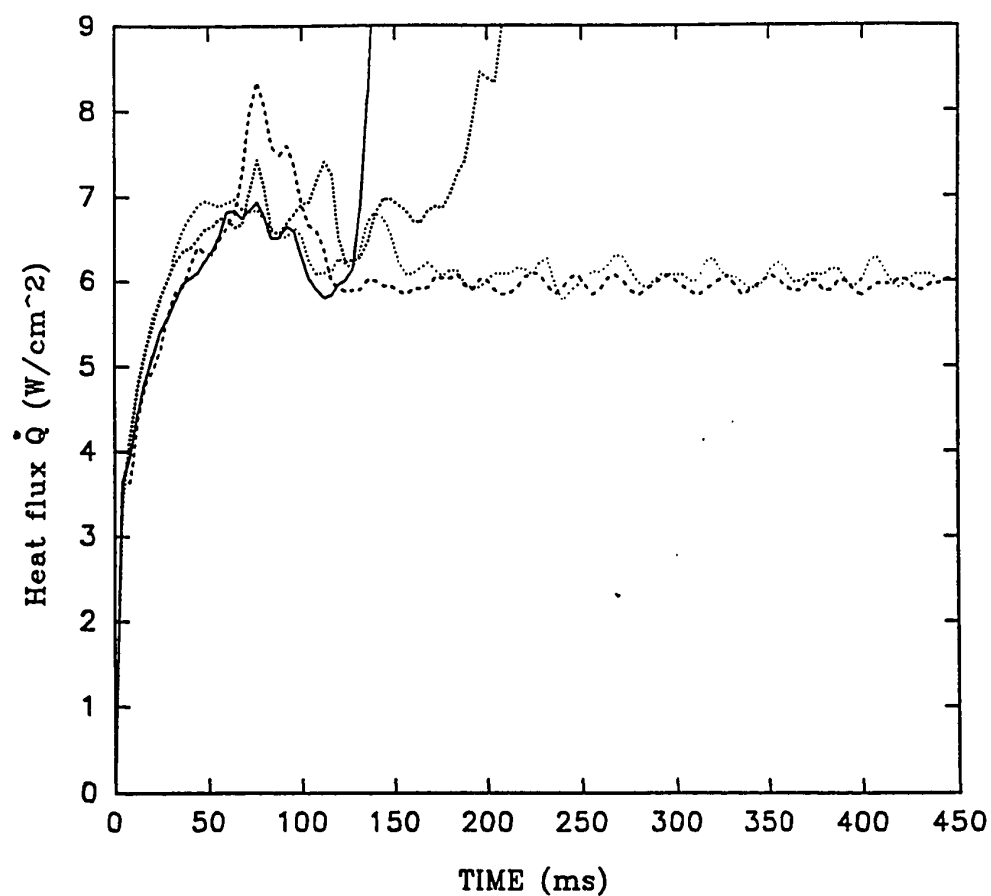


Figure 6. Heat flux  $\dot{Q}$  vs. time with forced convection. The heat flux as a function of time is shown for the platinum wire for four "identical" heat pulses and flow rates. The initial applied power is  $5.4 \text{ W/cm}^2$ . The flow rate is  $21.7 \text{ cm/sec}$ . Plot was derived from same data set as Figure 4.

film boiling occurs at power levels nearly 30% of the steady state value. This is the premature transition to film boiling referred to earlier. Moreover, a specific value of the transient critical heat flux or the superheat temperature for which film boiling inevitably occurs does not appear to exist. This suggests that other degrees of freedom are necessary to specify the state and evolution of the system.

#### STAINLESS STEEL RIBBON RESULTS

Qualitatively, the superheat vs. time curves for the stainless steel looked similar to the platinum wire curves. See Figure 7 for a comparison of the three heater/thermometers used. These curves were at power levels corresponding to their peak transient nucleate boiling heat flux, or  $p_{crit}^{tr}$ .  $p_{crit}^{tr}$  is defined as the maximum heat flux level attainable under transient and no flow conditions, in which film boiling did not occur.

Figure 8 shows the effects of various flow rates at a fixed applied current for the stainless steel geometry. The premature transition to film boiling occurs under zero flow condition at 75 ms and with increasing wire velocities this transition was delayed. Finally, at a high enough velocity film boiling was prevented. This pattern of increasing the delay to film boiling was obtained for higher power levels as well. However, the maximum one was able to delay film

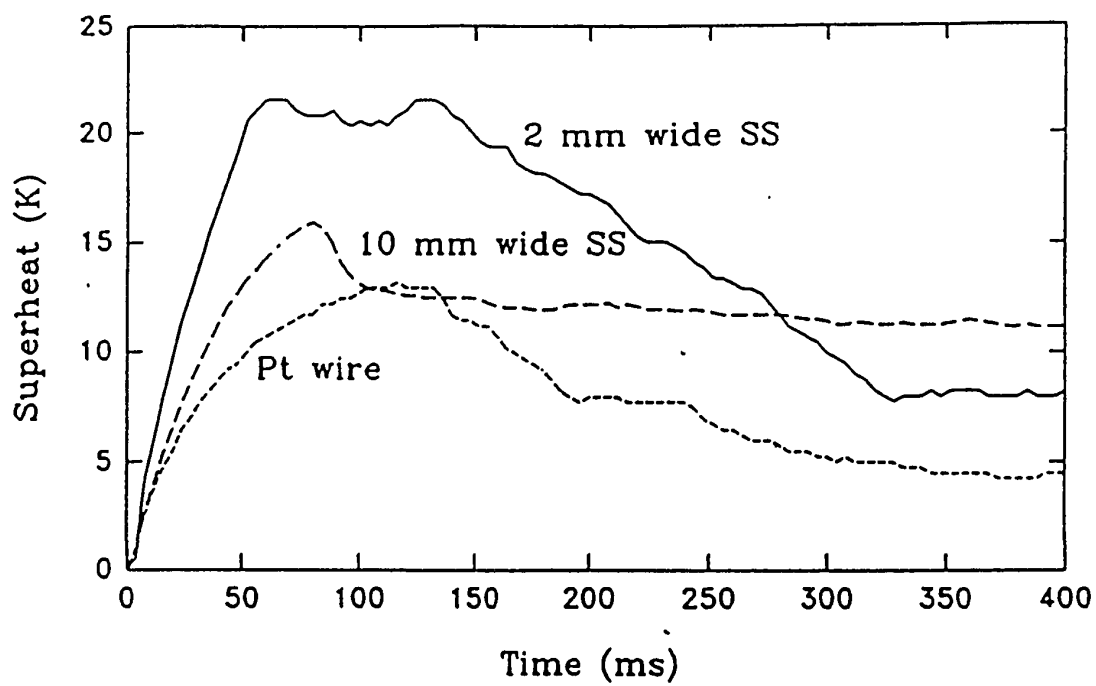


Figure 7. Superheat temperature  $\Delta T$  vs. time without forced convection. The temperature response as a function of time of all three heater geometries utilized. Applied powers are at their respective critical transient heat flux.

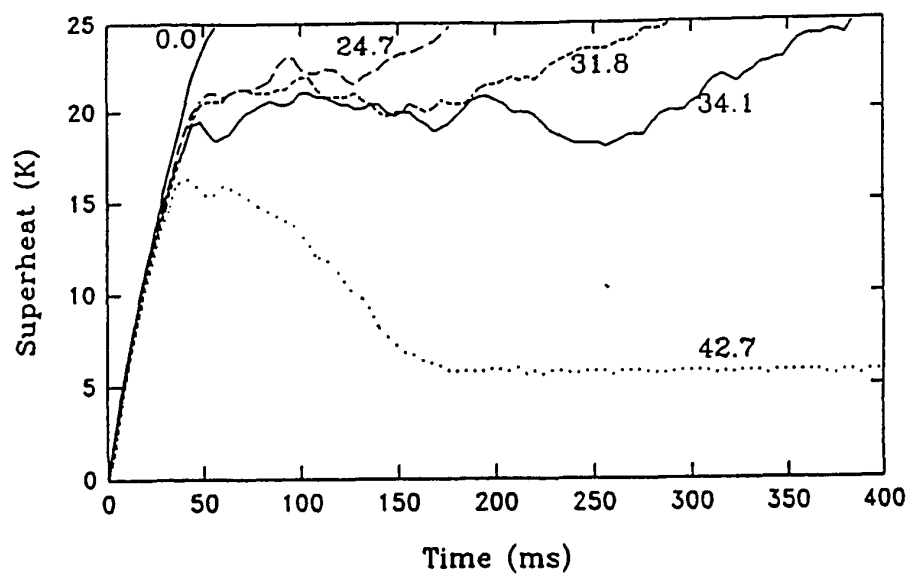
boiling if it was going to occur at all, was a few hundred milliseconds. Superheat plots and delay times under flow conditions similar to Figure 8 were also true for the platinum wire.

Table I gives a summary of the pertinent results on the various power levels attained for both the stainless steel and platinum heater/thermometer configurations. The effects of flow and transient heating are also included in Table I.

$p_{crit}^{ss}$  is the critical applied power per unit area under steady state conditions and no flow. It is also called the peak steady state nucleate boiling heat flux. This value was used as the baseline when making comparisons because it is the one typically quoted in heat transfer studies.

$p_{vmax}^{tr}$  is the maximum power level attainable in which film boiling did not occur under transient heating and maximum flow conditions. By looking at the ratios one can determine the severity of the premature transition to film boiling and the effect that forced convection had on suppressing it. The uncertainty in the reproducibility of the heat fluxes is plus or minus 0.1 W/cm<sup>2</sup>.

The difference in power levels can be understood as follows. In the case of the thin wire, the bubble size at departure was equal to, or greater than the size of the wire diameter. In effect, it only takes one bubble to surround the wire and initiate film boiling. The probability that this occurs is greater than if many bubbles



**Figure 8.** Superheat temperature  $\Delta T$  vs. time with forced convection. The temperature response of the 2 mm wide stainless steel heater is shown for an applied power of  $8.1 \text{ W/cm}^2$ . The numbers adjacent to the curves indicate the velocity of the wire in cm/sec.

TABLE I  
POWER LEVELS FOR VARIOUS CONFIGURATIONS (IN W/cm<sup>2</sup>)

Heater Configuration	$P_{crit}^{ss}$	$P_{crit}^{tr}$	$\frac{P_{crit}^{tr}}{P_{crit}^{ss}}$	$P_{vmax}^{tr}$	$\frac{P_{vmax}^{tr}}{P_{crit}^{ss}}$
0.2 cm wide steel ribbon	10.4	6.7	0.70	8.7	0.84
1.0 cm wide steel ribbon	6.3	4.8	0.77	6.7	1.06
.01 cm diameter platinum wire	9.6	4.0	0.42	6.6	.69

are required to coalesce into a film. Therefore, fewer bubbles (ie. lower power levels) were necessary to initiate film boiling with a thin wire than with an extended ribbon style heater surface. This mechanism holds whether transient or steady state heating was occurring. The reason this argument does not seem to hold for the largest heater (ie. the 1.0 cm wide heater) was because of other effects that dominated. These other effects were the confined dewar geometry in conjunction with the large total power dissipated into the liquid. The total power dissipated into the liquid was greater because of the greater total surface area of the wide heater. Consequently, visual observations indicated that much more boiling was occurring in the dewar than when the platinum wire was used. Because of the confined geometry, normal convective flow was impeded by the large high density of bubbles and film boiling resulted at

lower heat fluxes. The effect of dewar geometry on the critical heat flux was not anticipated; however, a more detailed study was initiated and is discussed in a later section.

Figure 9 shows the effect of flow on eliminating the premature transition to film boiling. The plot is  $\frac{P_v^{tr}}{P_{crit}^{ss}}$  vs. wire velocity  $v$  for all three of the heater geometries used.

$P_v^{tr}$  is the maximum threshold power below which the transition to film boiling never occurred when the wire velocity is equal to  $v$  and  $P_{crit}^{ss}$  was previously defined. It is important to keep in mind however, that the power levels plotted are a lower limit for a particular flow velocity. These data obviously do not lie on a straight line; it is not certain whether the data should follow a linear or quadratic power law. The lines drawn through the data are to guide the eye and are the results of a graphing routine. It is not to be implied that these data have been fitted with some simple polynomial. However, the curves are approximately parallel, which indicates that the flow has the same general effect on the various heaters. The actual values of the flow velocity required to prevent film boiling can be estimated with a model. Also, it is shown that gravity does not have much effect on these results because the same results were obtained regardless of whether the heater/thermometer was moved up or down through the liquid.

A simple model based on a rigid sphere moving through a

viscous fluid of a different density was used to analyze the forces on the bubbles. It was found that the viscous drag forces were larger than the buoyant forces due to gravity (Equations 9 and 10 below). This is true for bubbles whose radius was smaller than 0.1 mm which was the case when nucleation commences [20]. In other words, the bubbles were sheared away from the surface by the viscous forces before they could grow and coalesce into a film surrounding the wire. The viscous drag force calculated was based on the model of a rigid sphere moving through a viscous fluid having a different density relative to the sphere [21]. Here, the sphere is a vapor bubble of nitrogen and the viscous fluid is LN2. The drag force is:

$$F_d = 6 \pi a \eta v \quad (9)$$

where  $a$  is the radius of the sphere (bubble), which was estimated to be 0.01 cm from visual observation,  $v$  is the velocity of the heater/thermometer through the fluid, and  $\eta$  is the dynamic viscosity of LN2 at 77 K ( $1.58 \times 10^{-3}$  g/cm-sec).

The buoyant force on the bubble is given by

$$F_b = (\rho_{fluid} - \rho_{bubble}) g \frac{4}{3} \pi a^3 \quad (10)$$

where  $\rho$  is the density of the different phases (0.807 and 0.004 g/cm<sup>3</sup> for liquid and vapor respectively),  $a$  is the radius of the bubble, and  $g$  is the gravitational acceleration (980 cm/s<sup>2</sup>). Calculations were made on the

velocity necessary to prevent film boiling at a particular power level. It was determined that one has to replenish the liquid near the surface fast enough so that the bubbles forming cannot coalesce into a film. This amounted to moving the wire through a distance equal to its length in the amount of time required for the stationary wire to go into film boiling. For instance, from Figure 2 at an applied power of  $2.7 \text{ W/cm}^2$ , it is observed that the time until film boiling is 250 milliseconds. Since the wire length is 10 cm, the required velocity is 40 cm/sec. This result is within a factor of two of the experimental data if one extrapolates the curves in Figure 9 to the point such that  $\frac{p_v^{tr}}{p_{crit}^{ss}}$  equals one.

#### DEWAR GEOMETRY

As suggested above the dewar geometry and heat leak into the dewar affect the values of the critical heat flux and the severity of the premature transition. The former is true because the geometry determines the boundary conditions for any convective flow of the fluid. A confined geometry tends to restrict fluid and bubble flow away from the heater surfaces. This facilitates the transition to film boiling and one expects lower critical heat fluxes for the steady state case.

The effect of heat leak into the dewar was to contribute to the total heat flux (heater input plus heat

leak) that the fluid experiences. This enhanced the natural convection in the bath of LN2 which could aid in preventing a vapor film from forming. But if the heat leak is severe it can increase the density of bubbles near the heater and thus make film boiling more probable. This effectively reduces the critical heat flux of the heater.

With these effects in mind investigations were made utilizing dewars with different geometries and having different insulation properties. The dewars chosen were a 35 liter (40x35 cm) storage dewar, a 1 liter (30x7 cm) diameter glass dewar, and a 9 liter (45x5 cm) glass dewar. The 9 liter dewar was able to be placed inside a larger dewar containing LN2, thus reducing the heat leak considerably. Transient and steady state measurements without forced convection were made utilizing the platinum wire. The results are shown below in Table II. The symbols are as previously defined. The results confirm the qualitative discussion above. For example, all the configurations above except the second one had minimal heat leak into the dewars. This made for a very quiescent bath in which the premature transition to film boiling occurred at low power levels. Note these peak transient heat fluxes are all about  $2.8 \text{ W/cm}^2$ . The second dewar configuration had visible boiling and mixing of the liquid occurring. This caused the peak transient heat flux to be greater ( $4.1 \text{ W/cm}^2$ ) than the other configurations.

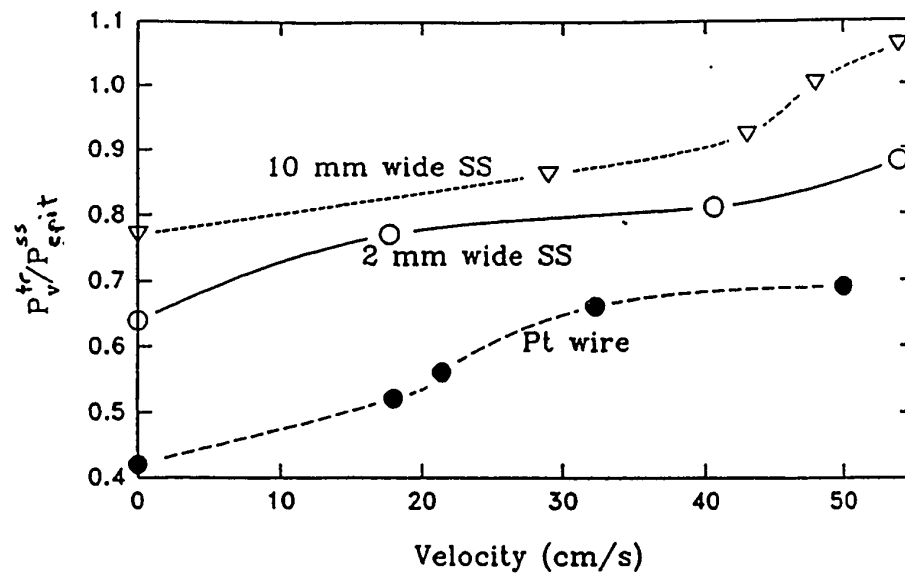


**Figure 9.**  $P_v^{tr} / P_{crit}^{ss}$  vs. wire velocity  $v$ . Effect of flow on the premature transition to film boiling for all three of the heater geometries used.

TABLE II

PEAK HEAT FLUXES AS A FUNCTION OF DEWAR GEOMETRY (IN W/cm<sup>2</sup>)

Geometry of Dewar	$p_{crit}^{ss}$	$p_{crit}^{tr}$	$\frac{p_{crit}^{tr}}{p_{crit}^{ss}}$
40x35 cm storage dewar	9.0	2.8	0.31
50x5 cm glass dewar(no LN2 bath)	7.4	4.1	0.55
50x5 cm glass dewar(in LN2 bath)	9.6	2.7	0.28
30x7 cm glass dewar	7.0	2.8	0.40

The steady state peak heat fluxes were affected both by the geometry and the heat leak into the dewar. The second configuration because of its large heat leak had many additional bubbles near the heater surface. This higher density of bubbles contributed to the lower peak steady state heat flux. Note that when a LN2 bath was placed around this dewar (configuration 3) the peak steady state heat flux is increased to a higher value. It was not so clear why the fourth configuration has its steady state value significantly lower (7.0 W/cm<sup>2</sup>) than all the others. From visual observation it did not appear that extensive boiling was occurring. It was possible that the heater surface was adjacent to the dewar wall and thus preventing the bubbles from dispersing easily.

## SUMMARY

The first half of this study attempted to answer some questions in heat transfer that are of direct interest from a practical viewpoint. Such questions concerned the critical heat flux through the heat/fluid interface and the typical superheat temperatures attained. This research expanded traditional studies of engineering heat transfer in a few ways. One, a cryogenic fluid was examined under transient as well as steady state heating conditions. Two, the effect of geometry in both the heater and dewar assemblies was determined.

To summarize the results: Transient heating of a solid immersed in LN<sub>2</sub> was found to cause a significant reduction in the critical heat flux into the liquid. This reduction could be to as little as 30% of the peak steady state critical heat flux. The reason for this reduction may have been the lack of well developed convection currents in the liquid; in a transient heating experiment there was not enough time for the quiescent bath to develop convection currents. This explanation was further supported by the observation that the dewars having enough heat leak such that mixing was occurring, had higher peak transient heat fluxes.

The effect of very thin heater geometries (eg. wires) was to aggravate the premature transition to film boiling. One explanation was that the bubble size was equal to or

greater than the heater diameter. Thus it only took one bubble to initiate film boiling.

Experiments utilizing forced convection were done to quantitatively determine the equivalent effect of natural convection. Predictions extrapolated from the results indicate that flow rates between 0.5 and 1.0 meters per second were necessary to completely prevent the premature transition to film boiling. Fortunately, these flow rates are achievable (for instance from pumps or pressurization) for most practical situations. Furthermore, the added complexity of a forced convection system may often be justified by the more than 200% increase in transient peak heat fluxes. Unfortunately, the apparatus used in these experiments does not allow testing the 0.5 to 1.0 m/sec flow rates predicted above.

Boiling heat transfer in a confined geometry similarly reduced the beneficial effects of any natural convection. The resultant bubbles were not able to disperse freely and therefore coalesce into a film more easily.

Overall, these results add significant new data to the heat transfer literature and indicate that previously neglected questions in heat transfer are important after all. Hopefully, this course of inquiry will stimulate further research.

## CHAPTER V

### INTRODUCTION TO NONLINEAR DYNAMICS

As mentioned in Chapter I, the second phase of this research involved the fields of nonlinear dynamics, dynamical systems and chaos theory [22,22]. These areas have grown dramatically since their "discovery" a few decades ago and they have applications to nearly all branches of science and engineering. Actually, it was at the turn of the century that much of the work for these fields was initiated and developed by the French mathematician Poincaré. However, his work tended to be passed over by physical scientists as arcane and unrelated to the types of systems they studied or the mathematics they required. Its importance was not recognized until the early 1960's when a meteorologist named Lorenz was attempting to model convective air flow in the atmosphere with a set of nonlinear coupled differential equations [24].

Lorenz observed in the solutions to his set of equations what is now commonly called extreme sensitivity to initial conditions. This effect causes two states that are infinitesimally close to each other at one point in time, to evolve to states that separate exponentially in time. This behavior does not occur in linear systems of equations. For

coupled linear equations, if one begins with two initial conditions that are close together, then at any future point in time the trajectories of the two solutions will diverge linearly in time. It is the linear systems which most scientists are trained in and therefore one of the reasons their intuition breaks down when encountering nonlinear phenomena. The ramification of Lorenz's results is that one eventually loses the ability to predict the future evolution of the system even though there exists deterministic equations that govern the system. Furthermore, this unpredictability and complexity is not a result of stochastic variables in the equations or due to a large number of complex equations. Lorenz's equations are just a set of 3 first order nonlinear differential equations. The conclusion drawn is: *complex behavior does not require complex systems.*

With this new knowledge in hand it might be wise to go back and look at some physical systems, that previously were thought to be too complex, in a new perspective that these fields afford. One hopeful candidate is the field of fluid dynamics, in which turbulent fluid flow is almost a totally unsolved problem [25]. But, one might wonder what would be the point - since one eventually loses all predictability as the system evolves? Actually all is not lost, there are a few characteristics about the system that can still be useful but which will be explored in later sections.

The connection of this to the present studies in boiling heat transfer is as follows. Boiling heat transfer is a complex process in which erratic fluctuations in temperature of the heat transfer surface are observed. It is possible that there is some simple underlying dynamic describing the system, and that some useful information can be extracted. The following describes how some aspects of heat transfer are operationally practiced and indicates a need for improvement.

Typically, when data for maximum boiling heat fluxes are needed for a specific design configuration one has to rely on data from others that were most likely taken under slightly different circumstances. As a result, the values used are little better than order of magnitude estimates [4]. Ideally, one wants to know more precisely what the maximum boiling heat flux is for a specific system so as not to have to overdesign the system for what might be well beyond worst case performance. Also, it would be beneficial to know whether any of the heat transfer parameters tend to change with aging or wear of the whole apparatus. There is no precise analytical method to analyze this, but it is hoped that by observing the right variables and using the appropriate analysis such knowledge may be inferred. Currently, the "correct" variables and analysis (if any) are not known; the goal here is to obtain some information after demonstrating the motivation for this line of inquiry.

At first glance, observation of boiling phenomena leads one to believe that the formation of bubbles on a surface and their subsequent departure is a stochastic process. Upon closer examination however, one sees that the bubbles always form at particular sites. These are called nucleation sites and their origin is thought to be in microscopic cracks and crevices in the heated surface. In these cracks are tiny pockets of trapped vapor that are the "seeds" for bubble formation. If heated, the bubble grows large enough to overcome the surface tension of the liquid and departs from the surface. However, a small portion of the vapor phase still remains in the crack and thus initiates the cycle again. Since most surfaces are not microscopically smooth, the distribution and size of these crevices vary, even between two surfaces that have been "identically" prepared. Quantifying this surface roughness is not very precise either. The reason surface roughness is important is because cracks of different size do not form bubbles with equal ease. That is, larger pockets of trapped vapor tend to form bubbles at lower surface superheats than smaller ones [13]. Consequently, it appears that even if one nucleation site can be crudely modeled, if there are thousands of these sites on a heater surface then heat transfer calculations will be extremely difficult. However, if these sites are not entirely independent, that is if they can communicate with each other, then their behavior might

reduce down to a simplified set of patterns. An example of this type of behavior is a set of nonlinear oscillators which all have slightly different natural frequencies when isolated, but which can mode lock to a single frequency when weakly coupled. For the system under study a few modes of coupling have been identified, one of which is heat transfer by conduction along the heater. For example, the site where a bubble forms is temporarily cooler than adjacent sites as the bubble absorbs heat due to the heat of vaporization of the liquid. Since this portion of the heater is now cooler than other locations, heat flows from adjacent areas to the bubble site. In effect, the other locations now "know" what is occurring at the bubble site. Another form of coupling is due to the bubbles themselves. Since the vapor has a much lower thermal conductivity than the liquid, the bubble acts as an insulating layer between different portions of the surface and the liquid. This interferes with the conduction of heat through the liquid. Also the bubbles, when in motion, act to mix the liquid in a form of convection which enhances heat transfer. These last two points were pronounced in my system because the heater surface was oriented vertically and thus the bubbles tend to drift along the heater wire. These considerations, and possibly others, suggested that coupling between different locations on the heater exists. However, it is not clear how strong this coupling was. There is also photographic

evidence from Tsukamoto that the bubbles form and depart in a regular way from a heated wire and thus are not random [5].

After a review of some of the main concepts of nonlinear dynamics and chaos theory in Chapter VI, a review of the methods for analyzing experimental data is presented in Chapter VII. In Chapter VIII the experimental results are presented, analyzed and discussed.

## CHAPTER VI

### REVIEW OF RELEVANT DYNAMICAL CONCEPTS

In this Chapter I introduce definitions and concepts used to describe a dynamical system from a qualitative, and geometric point of view. The term dynamical models or dynamical systems is meant any variety of systems (eg. physical, chemical, biological etc.) that can be modeled by various mathematical forms, be it differential equations or difference equations (mappings) [25]. At first, one might wonder - what is to be gained by describing a system from this alternative, geometric point of view? First, it is not practical to follow the time evolution of equations that exhibit extreme sensitivity to initial conditions (ie. are chaotic). Second, it is not always possible to construct even a crude model for the system. However, there are other compelling reasons as well.

Traditionally, one attempts to describe mathematically a physical system by writing down the best possible set of differential equations, although this is sometimes only a very crude approximation. The problem is "solved" if one can produce results either by analytical solutions or numerical computation, such that the results match observation within some limited domain [23]. In some

situations this might be a confining and misleading definition, in the same way that one has solved (at least in principle) all of physics because we can write down the Schrödinger equation in quantum mechanics or Newton's equation in classical mechanics. Condensed matter physics or chemistry might not have progressed as far if it had adhered to this point of view. Many interesting and practical phenomena such as phase transitions, though consistent with the fundamental equations of physics and chemistry, are not readily inferred from them. So even if the analytic solutions are known to some to reasonable approximation, reams of numerical output might obscure some of the global features of the system. Colloquially speaking, one cannot see the forest through the trees. Alternatively, the analytic solution might not be known and thus other options should be found. One option is that a system can be analyzed by examining its evolution or trajectory in state space, much as one would do in statistical mechanics [27]. Here, a more general definition for phase space is used than the one generally applied to phase space of a Hamiltonian system (ie. one with non dissipative interactions). In Hamiltonian systems one uses the canonical momentum and position as the variables. State space is a space where each axis represents a given physical variable and its position along the axis represents the magnitude. The number of axes can be any integer value and

represent any physical quantity. For example, a gas could be represented by a 3 dimensional state space of pressure, volume, and temperature, where a point in the space contains all relevant macroscopic information about the system at one instant in time. Although it might be easy to write down the relevant variables involved for a system, knowing the interactions involved between the variables, and how this causes the system to evolve over time is usually not trivial and one has to resort to experimental means to determine the allowable motion in this space. One of the advantages of viewing the system in its state space representation is that time need not be an explicit variable - it has been parameterized out. All one knows is the possible relationships that the variables may have with each other. What one wants to know is the "trajectory" the system follows as it evolves in this state space. By observing the patterns of this trajectory one can make qualitative observations on the behavior of the system as a function of some external control parameter. For example, is there an oscillatory component to the motion or is there some maximum value that a variable cannot exceed? For dissipative systems there is a surface in this multidimensional state space to which all trajectories are eventually attracted after any initial transient motion. (If energy dissipation occurs then it is assumed that there is some form of energy input driving the system, otherwise any motion would die

out.) This object or surface is called an attractor, and for a given system its exact shape or size might depend on the specific values of any of its parameters [28]. In general, the initial conditions do not have an effect on the attractor to which the trajectories converge, that is, the system loses "memory" of its initial conditions. However, it is possible that if one prepares the system to have two widely different starting conditions, the trajectories end up on two *different* attractors. Thus the region of initial conditions that converge to a particular attractor is appropriately called the basin of attraction for that attractor. A special type of attractor that is representative of chaotic systems in general, is a strange attractor. The word chaotic or chaos will be used here as the abbreviated form of the more precise term deterministic chaos. This term describes irregular or complex behavior of a system that is generated by deterministic, not stochastic equations. One characteristic that qualifies an attractor as strange is the concept mentioned previously, extreme sensitivity to initial conditions. That is, any two points which initially start off close together on the attractor become spatially separated at a rate that is an exponential function of time, although both trajectories have to remain somewhere on the attractor.

Another property of the strange attractor is that the dimension is generally fractal [29, Mandelbrot]. That is,

the dimension of the attractor in the phase space is non-integer and the patterns of the attractor may look self-similar at many different length scales.

When dealing with "objects" or a set of points in phase space it would be useful to have a method of characterization that yields quantitative results so that comparison with other sets of points can be made. One such geometric characterization is the dimension of a set of points. Many people have an intuitive feel for the notion of dimension when dealing with a continuum. For example, most would acknowledge that a line segment is one dimensional or that a solid sphere is three dimensional. Also, the value of the dimension for a system can be understood as the number of terms necessary to specify the coordinates of any point in state space for the system. Figure 10 shows a schematic indicating how the concept of dimension may be inferred by the spatial relationships between various points. The exponent  $\nu$  indicates how the number of points  $N$  contained within a given radius  $r$  scales (increases) with increasing radius. The dimension is this exponent. There are some variations in the specific form of these dimension algorithms but they are usually based on how a parameter, (eg. the number of points) scales with distances in the state space [28]. The caption of Figure 10 shows some of these relationships explicitly. In order to extract the scaling exponent  $\nu$  from the scaling

relationship:

$$N(r) \sim r^{\nu} \quad (11)$$

one makes a plot of  $\ln N$  vs  $\ln r$  and takes the slope. It is possible to calculate the distance between points even though the state spaces that one usually analyzes are not comprised simply of coordinates representing real spatial positions. This rule for calculating distance is called a metric. The most familiar metric, is the Euclidean metric. The Euclidean distance between any two points  $i$  and  $j$  is given by:

$$D_{ij} = \sqrt{(x_i - x_j)^2 + (y_i - y_j)^2 + (z_i - z_j)^2} \quad (12)$$

This example is only given for three dimensions, however and it is can be generalized to larger integers for any metric defined. Another metric, that and has been shown to be equivalent to the Euclidean metric, is the "taxi cab" metric (since it measures distances in blocks) [30] given by:

$$D_{ij} = |x_i - x_j| + |y_i - y_j| + |z_i - z_j| \quad (13)$$

The reason one uses the taxi cab metric (as opposed to the Euclidean) is that it is computationally more efficient. As demonstrated later, in some analyses calculations can take hours to perform. The dimension algorithm that will be used yields the correlation exponent or the correlation dimension. In analogy with Equation 11, the scaling relationship is given by:

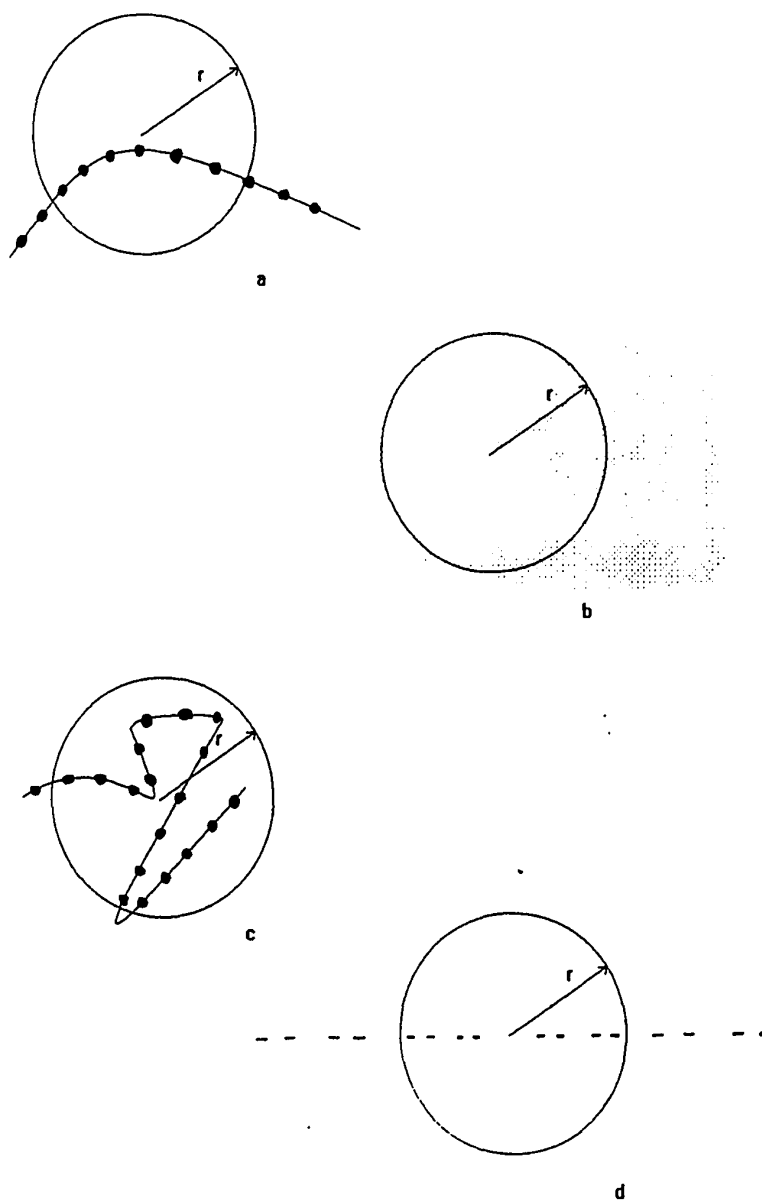


**Figure 10.** Dimension as a scaling parameter. The "area" is the number of points  $N$  within a circle of radius  $r$ . The area scales as a) line (dimension one)  $N(r) \sim r^1$ . b) surface (dimension two)  $N(r) \sim r^2$ . c) general case  $N(r) \sim r^v$ . d) Cantor set  $N(r) \sim r^{0.63}$ .

$$C(r) \sim r^v \quad (14)$$

where  $C(r)$  , the correlation integral replaces  $N(r)$  , the number of points. The correlation exponent is the slope of the  $\ln C$  vs.  $\ln r$  plot. The correlation integral is defined as:

$$C(r) = \lim_{m \rightarrow \infty} \frac{1}{m^2} \sum_{i,j=1}^m H(r - |\vec{x}_i - \vec{x}_j|) \quad (15)$$

Where  $H(r)$  is the Heaviside step function which has a value of one for distances between points  $i$  and  $j$  less than  $r$ , and a value of zero for distances greater than  $r$ . For each data point, a sphere or cube (depends on the metric chosen) of size  $r$  is constructed around that point and  $C(r)$  is calculated.  $C(r)$  is proportional to the number of data points that fall within that volume. This process is then repeated for several values of  $r$ . The result is that even if the system is such that the points plotted require a two dimensional state space, the scaling behavior of the number of points (ie. the area) with respect to the radius might be less than  $r^2$ , as would be the case for a solid two dimensional object. The process of calculating distances and correlation lengths can be generalized for systems that have phase spaces larger than two dimensions. As an example, Figure 11 shows the trajectory in the 2 dimensional phase space of the commonly studied Hénon attractor. This set of points was determined by the following 2 dimensional set of difference equations [31].

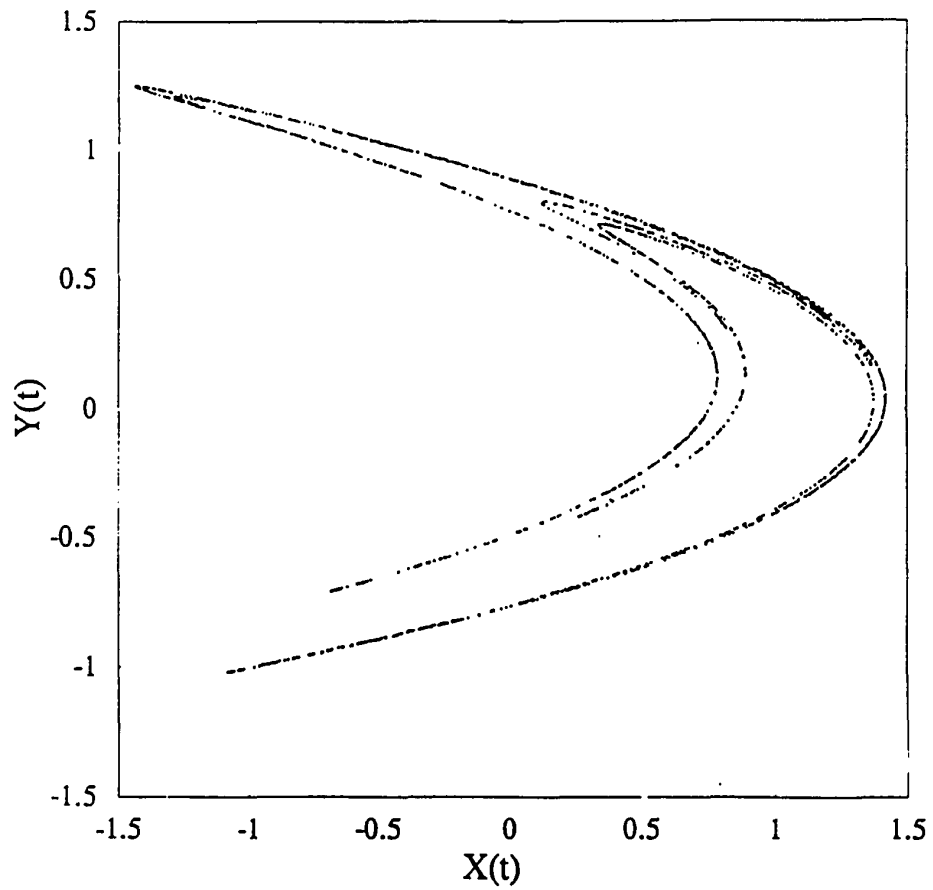


Figure 11. Hénon attractor. Plot of the trajectory for the Hénon equations, yielding the Hénon attractor.

$$\begin{aligned}x_{n+1} &= 1 - f x_n + y_n \\ y_{n+1} &= g x_n\end{aligned}\tag{16}$$

where  $f$  and  $g$  are constants. Calculating the correlation integral as a function of  $r$ ,  $\ln C$  vs  $\ln r$  was plotted in Figure 12. The slope was calculated from the middle portion of the line and is 1.26. This is in agreement with other investigators' results [20]. The ends of the curve were omitted from the slope calculation for two reasons. First, when only a finite number of points are plotted, at the small length scales there is a lot of empty "space" between points. The lack of a sufficient number of neighboring points yields poor statistics and thus a line that fluctuates. Second, at large length scales the correlation integral saturates to one. All the points are close together at this scale ie., from far away the attractor looks like a point.

Though there are other more complicated algorithms and statistical calculations which could have been used, this one is predominantly used when working with experimental systems. However, even for these simple dimension calculations there can be problems in determining unambiguous results for experimental systems. This problem is discussed in the next chapter.

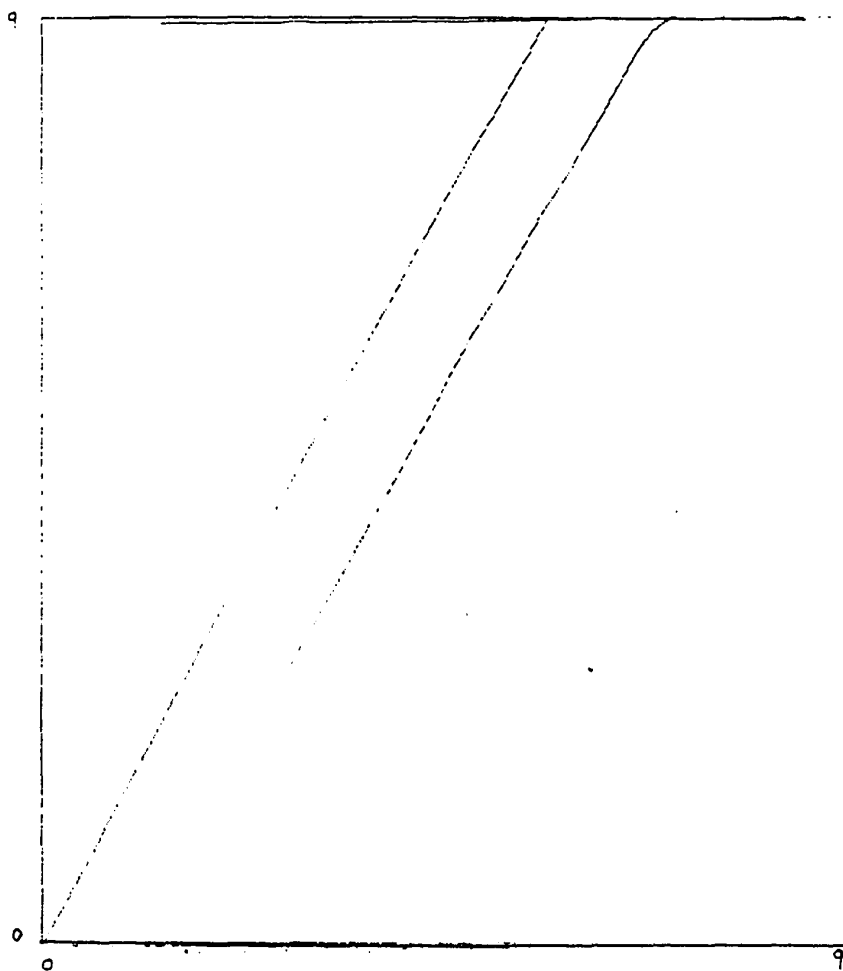


Figure 12.  $\ln$  of Correlation Length vs.  $\ln$  of Box size for the Hénon attractor. This is an example of how the slope of this plot yields the correlation dimension. The upper line is for reference and has a slope of 1.26. The lower curve is from the Hénon data.

## CHAPTER VII

### IMPLEMENTATION OF CONCEPTS IN AN EXPERIMENTAL SITUATION

The previous chapter introduced some of the concepts necessary to understand or describe properties of dynamical systems. But in all the examples, the equations that governed the dynamics were given explicitly. However, the experimental scientist does not typically have the equations of state at hand and might only have an imprecise knowledge of the relevant physical variables. (This discussion is based on the tacit assumption held by most scientists that there is *some* underlying set of deterministic equations governing the physical processes. Whether they are known or not is another question.) Furthermore, when one performs an experiment usually only one or two of the relevant physical variables are probed or sampled. The difficulty arises in obtaining phase plots of some natural phenomena when only incomplete information exists. There is a remarkable theorem by Dutch mathematician F. Takens that makes possible the connection between actual experiments and numerical experiments and mathematical analysis. This theorem says that one can still reconstruct a phase plot that in some way resembles the "true" phase plot by only having knowledge of one of the systems' variables [32]. By resemblance, it is

meant that the phase plots share some of the same geometrical or topological features, such as dimension. At first, this conjecture seems false: How can the dynamics of a multidimensional system be reconstructed from only one component. However, if these sets of equations governing the systems dynamics are coupled to each other, (see Equation. 16, the Hénon equations.) then one variable contains information about the other variables. The experimenter has to insure that the variable observed is one that is coupled strongly to the system of interest.

This "reconstructed" plot can be created by various techniques, but the one usually chosen by researchers is time series reconstruction by the method of delays [33]. Other methods involve taking multiple derivatives or integrals of the time series and using them to create the additional "independent" axes. However, taking higher derivatives of discretely sampled data can cause problems as the results will appear to change more abruptly than in the continuous physical case. To perform a time series reconstruction by the method of delays, one first takes a sequence of data from one of the physically relevant variables at equally spaced time intervals ie. a time series. This discretization process from the continuous variable can be represented as:

$$X_{(t)} \rightarrow \begin{bmatrix} x_{t_1} \\ \cdot \\ \cdot \\ x_{t_n} \end{bmatrix} \quad (17)$$

where  $t_n$  represents the time at which the  $n$ th data point is obtained. One then plots this series vs. itself, but at a later point  $\tau$ , in time. (See Figure 13 for a pictorial representation in 2 dimensions). This can be generalized to an  $m$ -dimensional vector by use of increasing time delays as follows:

$$\vec{x}(t_i) = [x(t_i), x(t_{i+\tau}), x(t_{i+2\tau}), \dots, x(t_{i+(m-1)\tau})] \quad (18)$$

In this way, a 1-dimensional scalar is embedded into an  $m$ -dimensional vector space. Since one does not usually know the dimension of the system under study, these "embedding" dimensions can be made increasingly larger until they exceed the true dimension of the attractor. This way, if the object (the reconstructed attractor) embedded has in reality a dimension less than the embedding dimension then, the calculated dimension will, too. An example of this is a line which still has a dimension of one whether it is drawn on a two-dimensional plane or in a three-dimensional volume. The only restriction of this embedding technique is that for some objects the embedding dimension used must be greater than  $(2d + 1)$ , where  $d$  is the attractor's true dimension [34]. Conversely, if the attractor's true dimension is greater than the embedding dimension then the calculated

dimension will yield the value of the embedding dimension.

Although this procedure is easy to implement, when working with a real data set which is limited in size and precision, the results can be less than conclusive. The reason is that Takens' theorem guarantees that the true and the reconstructed attractor are similar for a system in which an infinite amount of noise free data can be analyzed. It is unclear how well the reconstructed attractor converges towards the true one, for a noisy and finite set of data. Indeed, many experimenters have discovered how "good" the reconstruction is depends on the time delay chosen, noise level, and the total number of points evaluated [35,30]. Unfortunately, this problem is not resolved and to make things worse it is generally not possible to differentiate between systems *a priori* that are sensitive to the reconstruction parameters and the data and those that are not. What one does is analyze the data in a number of different ways, applying other researchers empirical findings as to which delays work best. Some of these findings by other researchers will briefly be discussed.

The first technique is to plot the autocorrelation function as a function of the time delay and find the first minimum. This function is defined as:

$$H(\tau) = \frac{1}{m^2} \sum_{i=1}^m x_i * x_{i+\tau} \quad (19)$$

This value of the time delay is then used in the phase space

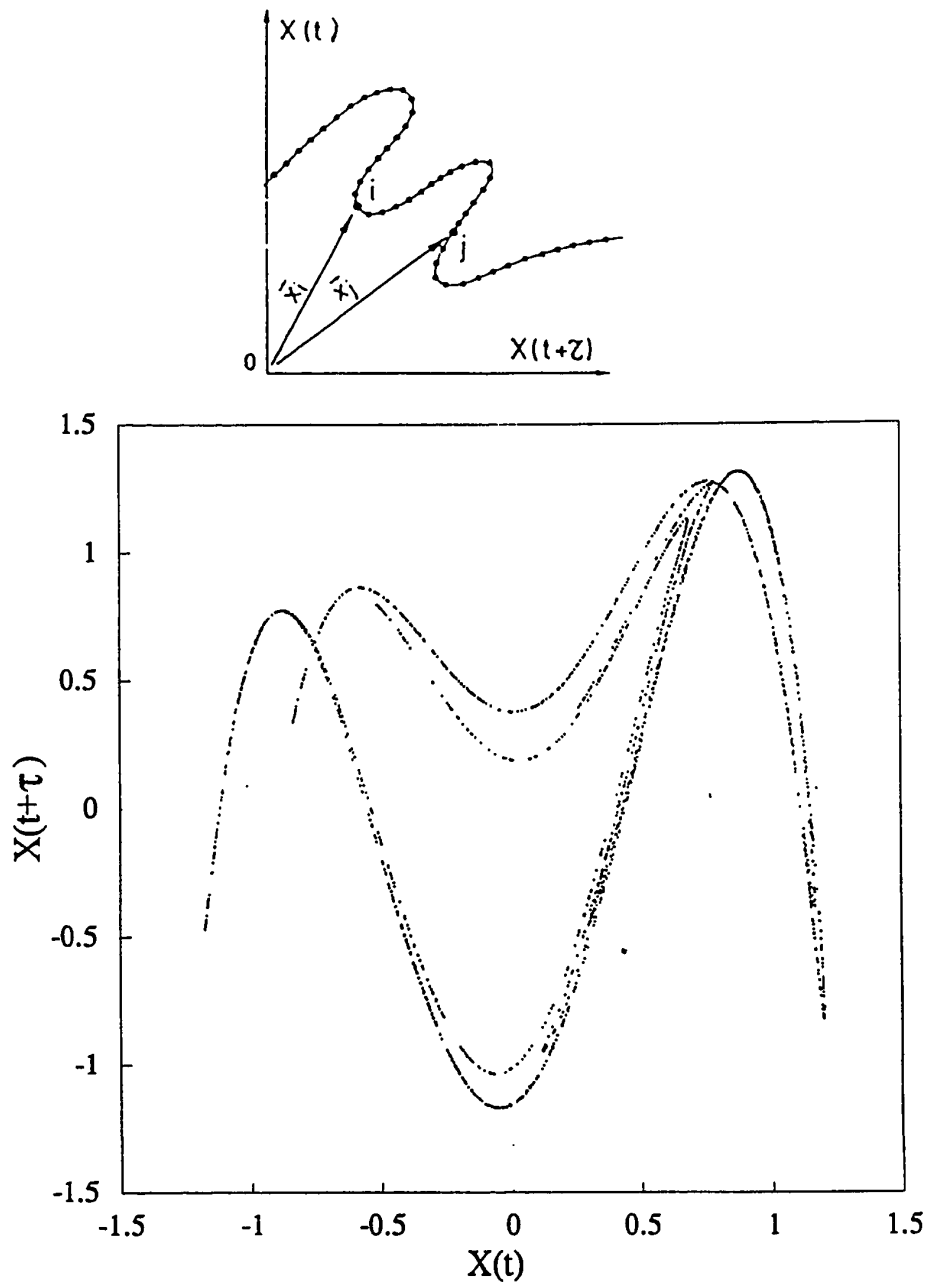


**Figure 13.** Phase space reconstruction of a time series by the method of delays. The upper curve illustrates the generic method. The lower curve illustrates the technique as applied to data generated by the Hénon equations.

reconstruction. If the time delays are too short (short is a relative term and depends on the behavior of the system under study), then the signal looks too much like itself (ie. nothing has changed). A phase plot in two dimensions would just be a diagonal line of  $y = x$ . If the delay is too long and the signal is chaotic, this indicates the signal at a later time will have no correlation with itself at earlier times (ie. all predictability is lost). A two dimensional plot of this would look like a random scatter of data. By locating the first minimum of the autocorrelation function, one evaluates the data at time scales in between these two extremes.

The other technique is to find the minimum of the mutual information function defined by Fraser [36]. For some systems this resulted in a better reconstruction than when the autocorrelation was used. The problem with using the mutual information is that it is rather cumbersome to implement. Other researchers have shown that plotting the correlation integral as a function of delay (keeping  $r$  fixed) and noting the first minimum, the same as the mutual information function [37].

Another concern when performing real or numerical experiments is the introduction of noise into the system. For numerical experiments the "noise" is a result of truncation and roundoff by the computer [35, 38]. Noise does not appear to be a major problem, but it would be

prudent to keep it as small as possible. Noise blurs the transition between different modes of behavior (ie. regular or chaotic) and the patterns in the phase plots fill out, thus obscuring any fine structure to the attractor [39]. This filling out process makes the underlying attractor appear to be higher dimensional than it really is. This is so because noise is "space filling", and by definition, has an infinite number of degrees of freedom, and thus dimensions.

The last significant problem to be addressed concerns real data sets and state space reconstruction is - how many data points are required to get a good reconstruction? This, like many of the other problems discussed, does not have a definitive answer and may depend on the specific system under study. Many authors have "derived" the minimum required data points for an accurate reconstruction [40,41]. The exact numbers and exponents may vary, but the required number of points  $N$  is thought to have an exponential dependence on the "true" dimension of the system. The estimates given range from  $N \sim 10^{d/2}$  to  $N \sim 42^d$ , where  $d$  is the attractor dimension. For example in six dimensions (which is not unreasonable for some physical systems) this translates to a minimum of 1000 points or a maximum of 5 billion. As one can see this is a large discrepancy and it is not possible *a priori* to decide which estimate to use. One empirical method to help decide this question is to

repeat the calculations with an increasing number of points and see if the results converge. The number of data required is an important practical question because some of the algorithms require iterations that scale with the square of  $N$ . If  $N$  is too large it takes a prohibitively long time to make the calculations.

As suggested, analysis of experimental data from some of the techniques previously mentioned can be problematic. The results can be inconclusive particularly when answers are sought to the absolute value of the dimension of the attractor. However, if one is only looking for relative changes in these quantities as a function of the system's parameters, then their utility is probably enhanced. In effect, the resultant calculations for a physical system would provide a "signature" for the ongoing processes, much like spectral analysis provides for linear systems. It is from this perspective of relative changes that my heat transfer data has been analyzed. It is hoped that this will provide a characterization of the approach from nucleate boiling to film boiling.

## CHAPTER VIII

### DYNAMICAL SYSTEMS RESULTS

A summary of the experimental configuration used for collecting the temperature and heat flux data is given. However, a more detailed discussion of the apparatus is found in Chapter III, because it is essentially the same set up as for Part I of this research.

A platinum wire of 0.1 mm diameter and 1 cm effective length was placed vertically inside the center of a double glass dewar, both of which were filled with LN<sub>2</sub>. The inner dewar is 5 cm in diameter and 1 m in length. An adjustable constant current source was connected to the platinum wire to provide heating. After low pass filtering at a cutoff frequency of 1 kHz (this frequency was determined from measurements of the temperature spectrum and aliasing considerations), the temperature signal from the wire was recorded for various steady increasing currents until film boiling commences. The fluctuating temperature data that were then analyzed. The maximum fluctuation was 0.5 kelvin, but the temperature resolution of the thermometer is a few millikelvins.

## FOURIER TRANSFORM RESULTS

The plots in Figure 14 are the amplitude of the Fourier transform of the temperature fluctuations. The three plots correspond to progressively increasing currents. The spectrum has a  $1/f$  shape and as the current increases the curve expands outward to include higher frequencies. Note this was not a spurious signal due to  $1/f$  noise commonly found in electronics, as evaluation of the background noise showed it to be a few hundred times smaller than the temperature signal. However, there did not appear to be any discernable characteristic frequencies for these three plots or any of the other data sets evaluated. This may not be informative as a chaotic signal may possess a few periodic components in addition to the required broadband spectrum. One form of chaos signified by the intermittency route to chaos exhibits a  $1/f$  spectrum [42,43].

The heat flux was calculated from the temperature data as was done in Part I of this research (see Equation 6) and its spectrum is plotted in Figure 15. Again, a similar but not identical,  $1/f$  pattern emerges. There was also a hump in the spectrum which moves outwards when the average power was increased. However, there did not appear to be any quantitative trend in either the amplitudes or frequencies of the heat flux spectrum as a function of heater power. The temperature and heat flux are some of the dominant variables that characterize this system. Apparently, the

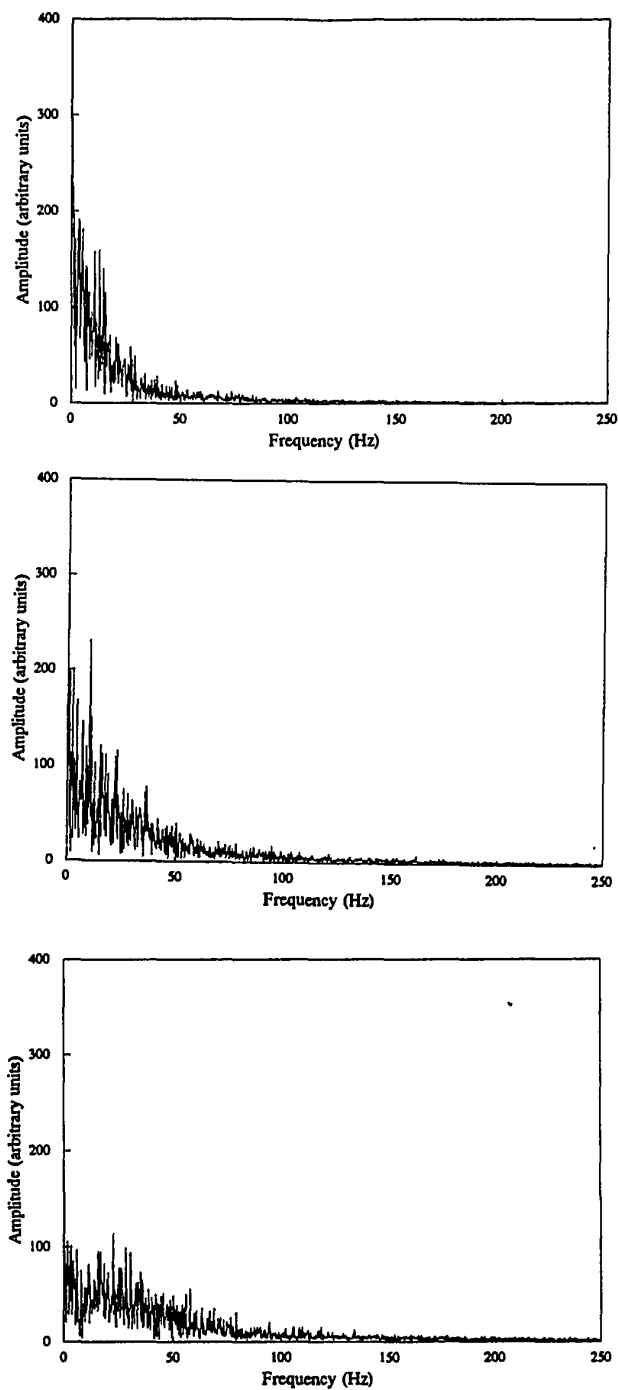


**Figure 14.** Amplitude of the fast Fourier transform of the temperature fluctuations. The three graphs correspond to different currents.

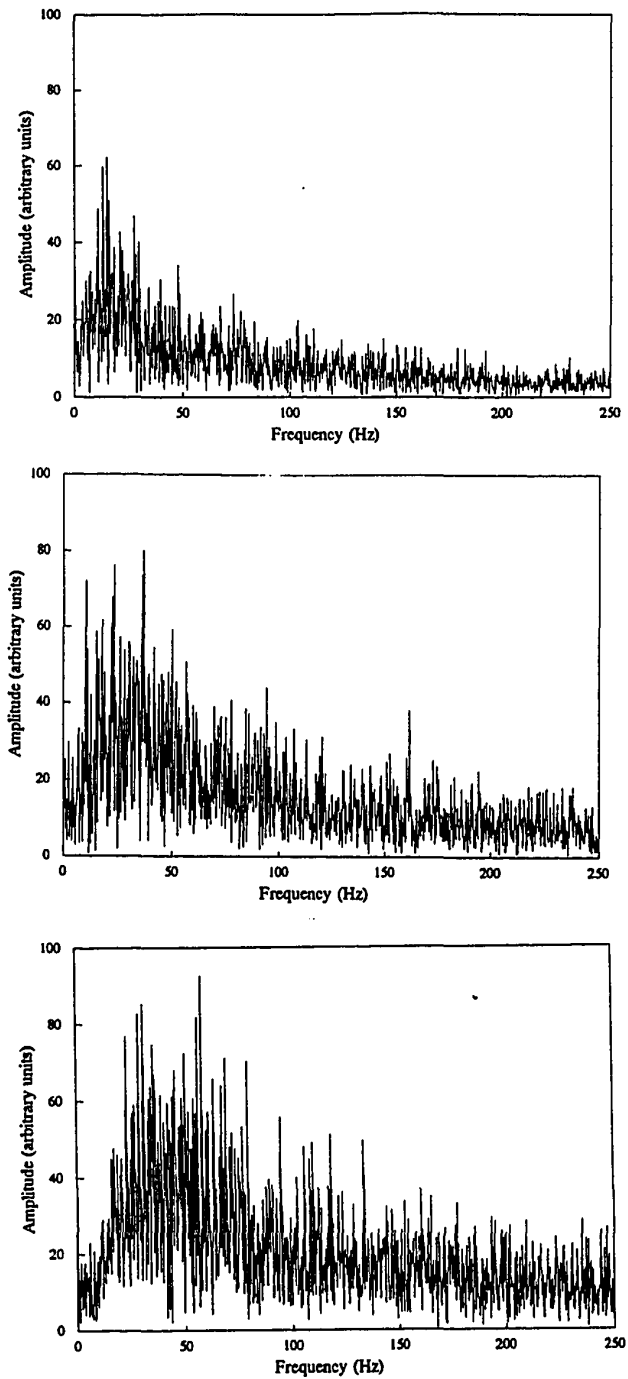


Figure 15. Amplitude of the Fast Fourier transform of the heat flux fluctuations. The three different curves correspond to different currents.

changing dynamics for the system are not sharply delineated by their Fourier spectrum.

#### PHASE SPACE RECONSTRUCTIONS

Next, a phase space reconstruction was done from a time series of the temperature data. The plots in Figure 16 are for embedding dimensions 4 through 10, and the time delay used for the reconstruction is indicated in the caption. Though the curves are generally straight lines, closer evaluation of their slope reveals a value that is nearly equal to their respective embedding dimension. This indicates that either the dimension of the attractor, *if there is one*, is higher than 10 or the data were dominated by noise. No attempt was made to evaluate these data in larger embedding dimensions because the number of data points required would have been prohibitive and the results suspect. These calculations were also made for a variety of time delays other than the ones suggested by the literature (results not shown). They too, all had slopes (dimensions) that do not indicate convergence to a low dimensional attractor, nor did they show any quantitative difference between the various power levels.

As mentioned, the most likely cause for not finding a low dimensional attractor was that this was not really a low dimensional system. Other experimentalists have calculated the minimum number of dimensions for an electrical system

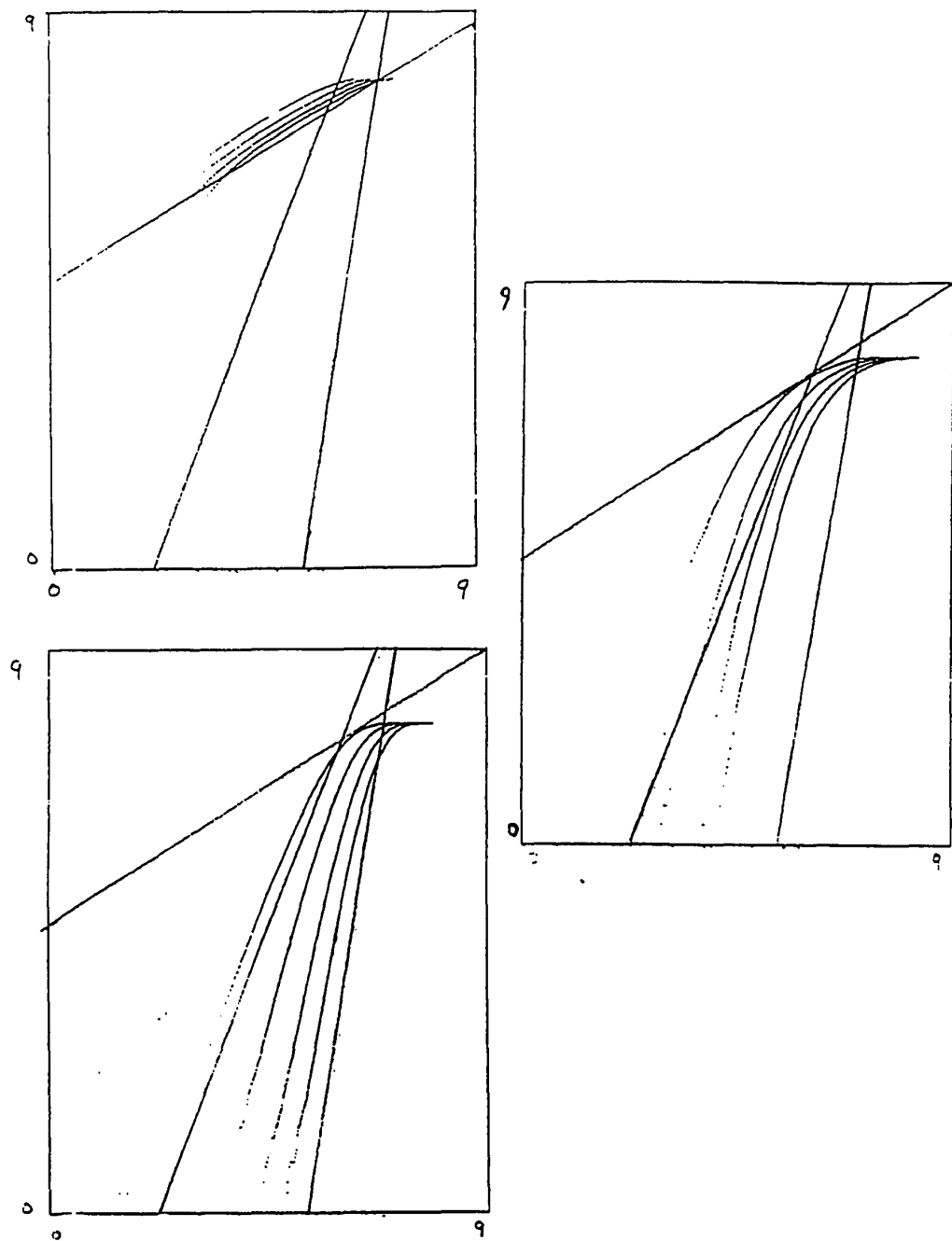


**Figure 16.** Ln of correlation length vs. ln of box size for the temperature fluctuation data. The three different curves correspond to different currents.

that exhibits a  $1/f$  spectrum to be more than 20 [43]. For the boiling heat transfer system, it was reasonable to assume the smallest unit or component comprising it is a single nucleation site. This bubble site contributed a minimum of one degree of freedom. From visual observation of the heater, the diameter of the bubbles at departure were 0.2 mm and the effective size of the heater/thermometer was 10 mm. Thus, depending on the heat flux, tens or hundreds of bubbles may have been originating on the wire. If these bubble sites were not strongly coupled to each other, then the effective number of degrees freedom was just the total number of bubbles, thereby precluding any low dimensional dynamics. It is not feasible to monitor a smaller boiling patch with the platinum wire for two reasons. First, the sensitivity of the thermometer decreases linearly with the length of the heater and would lead to a resolution that is too coarse. Second, end effects due to the current and voltage leads would interfere with the heating, boiling, and measurement processes.

There are additional experimental limitations that could have a detrimental effect. The dynamic range of the measurements was less than 55 dB because of noise. It is not clear how much this noise could be reduced. Also, a counter intuitive effect was that low pass filtering the signal could increase the dimension of a chaotic signal [44]. It was not clear what the optimal sampling rate, or

duration is for this system. If one were just interested in the temperature measurements, then sampling sufficiently above the highest signal frequency, might have been a good estimate. However, one is also interested in taking derivatives of the signal for plotting in phase space and this would increase the sampling requirements. Due to the A/D data acquisition system there was a limit to the number of points that can be recorded. Grossly oversampling to achieve smoother derivatives is not a viable option because of memory limitations of the computer. It did not appear that these problems could readily be solved; therefore an additional set of experiments with slightly different goals was performed. However, this will be presented in the Appendix.

#### FLUCTUATIONS IN THE $\dot{Q}$ - T PLANE

As mentioned, the heat flux and temperature are some of the important parameters characterizing the system. While the time dependence of these quantities appear to behave randomly, maybe there is a strong correlation between these two variables. Plotting the trajectory of  $\dot{Q}$  and  $T(t)$  could reveal some of their underlying dynamics. Figure 17 shows a sequence of plots for increasing power levels. The horizontal (temperature) axis range is 1 kelvin wide and the vertical (heat flux) axis range is 1 W/cm<sup>2</sup>. The offset is adjusted so that  $\dot{Q}$  and  $T$  are both centered on their

respective average values (not given). This indicates much more of a pattern than the previous results. It was difficult to tell from the static figure, but by observing the computer slowly plot the trajectory, the trace could be seen to be a crude ellipse which *on average follows a counterclockwise trajectory* about some average heat flux  $\dot{Q}_0$ , and average temperature  $T_0$ . The fact that this trajectory did not just show random fluctuations, was at first striking, and unexpected. This pattern seems to indicate an underlying dynamic. Therefore an attempt was made to construct a qualitative physical picture or model that is consistent with this motion. Also, an analysis of the relevant equations were made to see if they predict this motion.

Figure 18 shows a hypothetical trajectory in the  $\dot{Q}$ - $T$  plane along with a portion of the characteristic nucleate boiling curve superimposed. (The argument is qualitative so the actual units used and the exact shape of the curve were not calculated explicitly.) Also shown are the lines of constant average heat flux  $\dot{Q}_0$  and constant average temperature  $T_0$ . These lines intersect on the boiling curve. The sequence of points A through D represent the "life cycle" of a nucleation site on the heated surface, thus this was from a localized or microscopic point of view. At point "A" a bubble starts to form in the superheated liquid as power is continually dissipated into the wire.

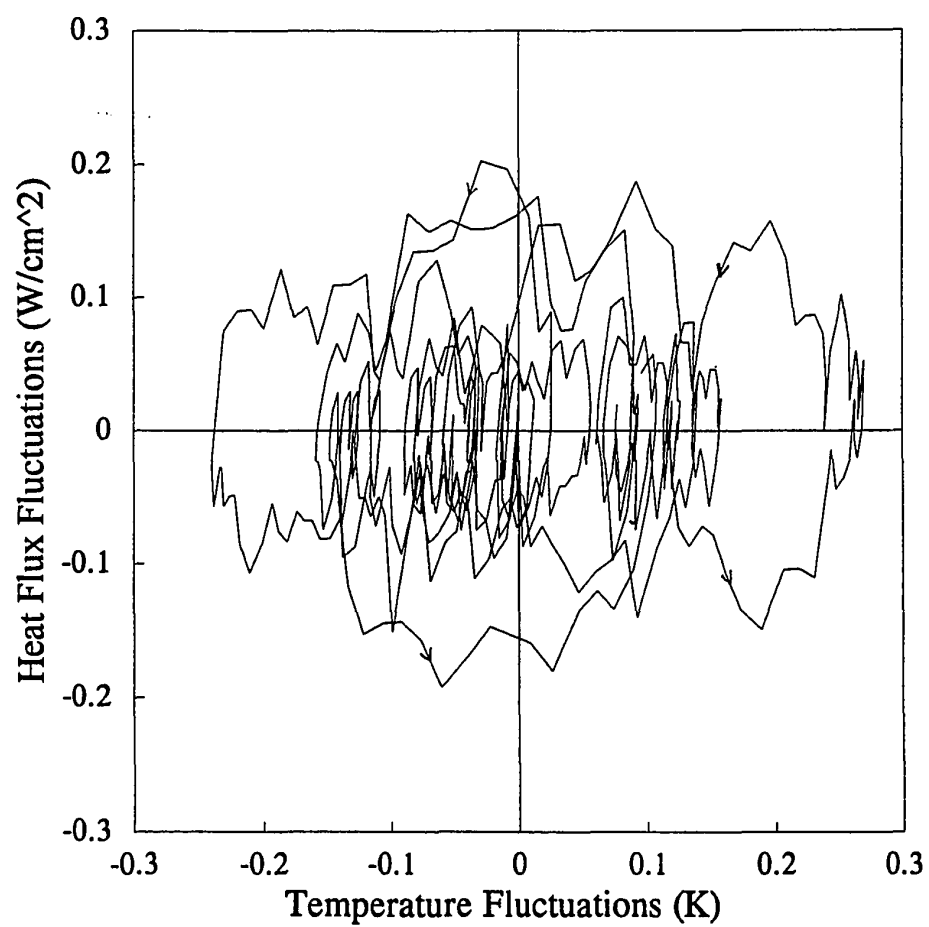


Figure 17. Fluctuations about the Steady State in the Heat Flux - Temperature Plane.

This absorbs some of the heat but does so isothermally (step A-B). When the bubble increases in size it begins to insulate the wire, thus diminishing cooling by means of conduction or convection and driving up the temperature (step B-C). Finally, the bubble becomes large enough that it breaks off and leaves the surface because of buoyant forces. The cold liquid then rushes in, thereby increasing the heat flux and decreasing the temperature (C-B-A). The process repeats itself as a new bubble starts to form.

While this last scenario is reasonable, it seems to predict that counterclockwise motion is the only one allowed. Observation of the experimental data indicate that while on average this is true, it is not rigorously true for every successive point. So, how does this apparent violation come about? The problem lies in the boiling curve drawn in the  $\dot{Q}$ -T plane. Typically, this empirically derived curve can be approximated by an equation which has the form:

$$\dot{Q} = h\Delta T^\alpha \quad \{ 1 \leq \alpha \leq 3 \} \quad (20)$$

where  $h$  is the heat transfer coefficient. This curve is not really a sharp line which remains stationary in time; it is an average. More appropriately, it can be thought of as a family of similar, closely spaced curves. The overall instantaneous state of the system determines which curve the system is on. That is, although the temperature and heat flux are the dominant variables in determining these boiling

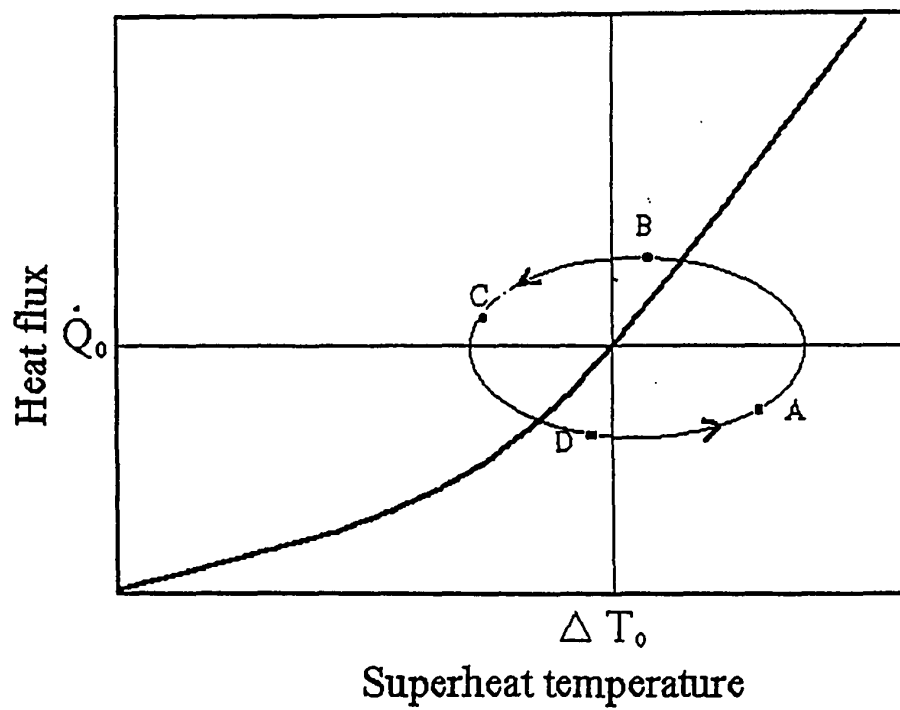


Figure 18. Life Cycle of a Bubble in the Heat Flux - Temperature Plane.

curves, there are other less important degrees of freedom as well. For example, how many bubbles surrounded the surface, or what was the local convective flow pattern? The true trajectory followed a unique path in some higher dimensional phase space which included *all* the relevant variables. A particular boiling curve was realized by "slicing" this higher dimensional manifold to the  $\dot{Q}$ -T plane. Different parallel "slices" correspond to different external conditions in the system or equivalently, to different times. In effect the system "sees" a time varying heat transfer coefficient.

Another, more analytical way to show this uses the conservation of energy concept. Referring to Figure 18 again, the  $\dot{Q}$ -T plane can be divided up into 4 quadrants. The constant  $\dot{Q}_0$  line and the boiling curve were the dividing lines. Energy conservation requires that the power input to the heater must show up as either heat flux  $\dot{Q}$ , out through the surface or, because of the nonzero heat capacity of the heater, as an increase in the temperature T of the heater. Mathematically this is stated (see Equation 6 for explanation of terms):

$$P = \dot{Q} + \frac{Cd\Delta T}{dt} \quad (6)$$

Given that the applied power is constant, the long time averaged steady state heat flux  $\bar{Q}$  is:

$$\bar{Q} = P = \dot{Q}_0 \quad (21)$$

where  $\dot{Q}_0$  is the steady state heat flux. The steady state temperature is denoted by  $\Delta T_0$ . One is interested in the variables  $\dot{Q}$  and  $\Delta T$  and their fluctuations about their steady state values. These variable are defined as:

$$\begin{aligned} \delta \Delta T &= \Delta T - \Delta T_0 \\ \delta \Delta \dot{Q} &= \dot{Q} - \dot{Q}_0 \end{aligned} \quad (22)$$

The time derivatives of these variables were examined to ascertain whether restrictions apply to their sign. Rewriting Equation 6 in terms of  $\delta \Delta T$  and  $\delta \dot{Q}$  gives:

$$\frac{d\delta \Delta T}{dt} = \frac{1}{C} (\dot{Q}_0 - \dot{Q}) = -\frac{1}{C} \delta \dot{Q} \quad (23)$$

This yields

$$\frac{d\delta \Delta T}{dt} = \begin{cases} < 0 & \text{when } \dot{Q} > \dot{Q}_0 = P \\ > 0 & \text{when } \dot{Q} < \dot{Q}_0 = P \end{cases} \quad (24)$$

Therefore, the line  $\dot{Q}_0$  is the dividing line which determines the sign of  $\frac{d\delta \Delta T}{dt}$ . The position in phase space relative to the steady state heat flux curve helped determines the sign of  $\frac{d\delta \dot{Q}}{dt}$ , but not in all four quadrants. In essence, the trajectory "wants" to return to the equilibrium heat flux curve. This allowed a trajectory in the first and third quadrant to have either a positive or negative  $\frac{d\delta \dot{Q}}{dt}$ . It will have to be determined by more sophisticated analyses and experimentation whether there is a physical preference. Because of conservation of energy, quadrants two and four require that  $\frac{d\delta \dot{Q}}{dt}$  be negative and positive respectively.

To carry this analysis further, one would like to distinguish quantitatively between the plots obtained at different average heat fluxes. One way of doing this is to calculate the "circulation" of these trajectories. That is, calculate the area in the  $\dot{Q}$ -T plane swept out per unit time by the trajectory. These calculations were made and plotted for various average heat fluxes on a computer. The results are plotted in Figure 19. Note the steady increase of the area with increasing heat flux. As one approaches the steady state critical heat flux it appears to level off and even decrease some. This peak may be the precursor to film boiling that has been sought after.

#### SUMMARY

The results in the latter half of this work has been successful and suggest that further study will yield more interesting surprises. As stated in the introduction, this part of the research took a path that utilized non-traditional methods of analysis in heat transfer. For example, the main items of interest were: how the system evolved in time and the characteristics of the fluctuations of the state variables  $\dot{Q}$  and T. On the one hand, an attempt was made to get answers for some practical questions. A novel explanation was found by observing that the "circulation" in the heat flux and temperature plane suggested when film boiling was approaching.

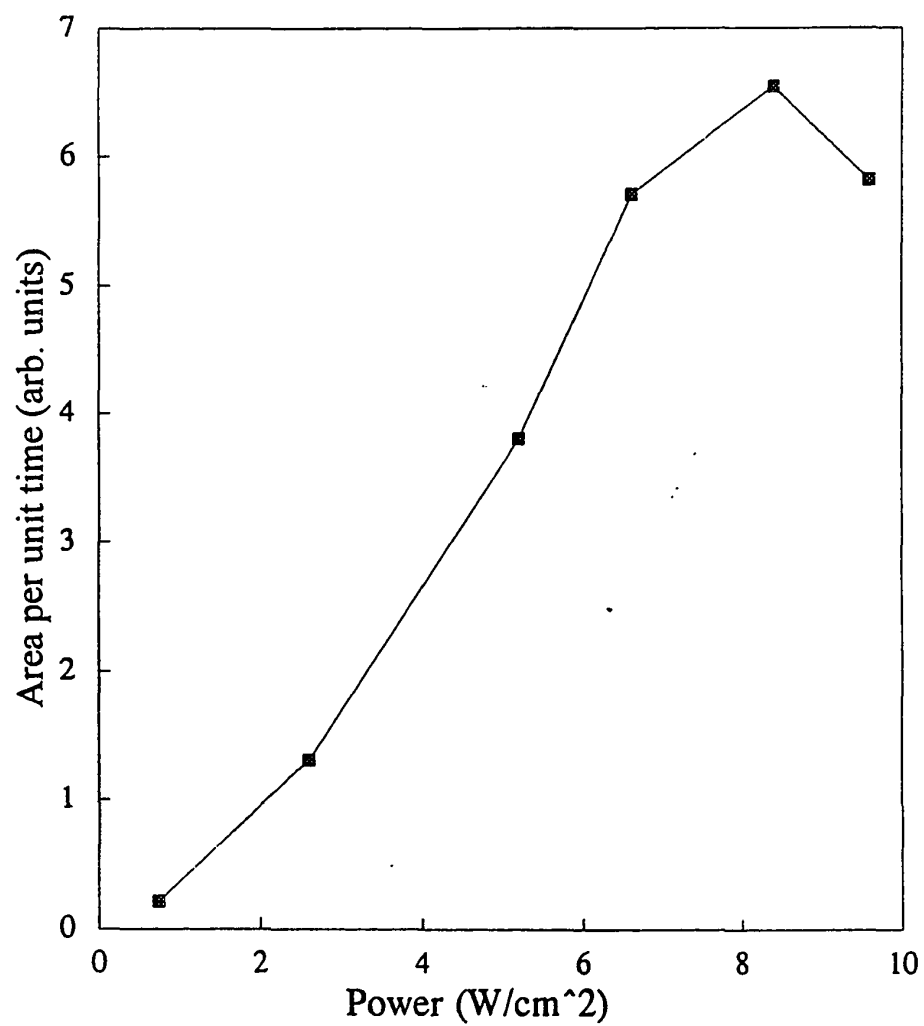


Figure 19. Area per Unit Time Swept Out in the Heat Flux - Temperature Plane.

On the other hand, some of the other analyses gave inconclusive results. But the structure observed in the Q-T plane is suggestive that more sophisticated experimental and analytical investigations may lead to an unequivocal determination that chaos is present. Also, this research produced some interesting and unanswered physics questions concerning the nature of nucleation. Analogous to the Faucet Drip Experiment, can single nucleation sites exhibit chaotic rhythms? (See Appendix) and " Do aggregates of these sites behave in some sort of collective manner which can be described by simple, low dimensional dynamics? " I hope that sufficient curiosity has been aroused, and the groundwork laid to insure that this line of research will be continued.

## CHAPTER IX

### CONCLUSIONS

This work was divided into two parts. The first part dealt with measurements of temperature and heat flux under conditions of steady state and transient heating. It was found that transient heating caused a 30% reduction in the critical heat flux compared to that of the steady state values. The reasons for this reduction was suggested to be the lack of well developed convection currents in the liquid. Consequently, forced convection was investigated to eliminate the premature transition to film boiling. The data indicated that flow rates of less than one meter per second were successful in suppressing the premature transition to film boiling. This was quite a significant increase (more than 300% in some cases) in critical heat flux.

Also, noting that slightly different heater and dewar configurations sometimes gave significantly different results, investigations were made to characterize these different parameters. It was determined that the heat leak into the dewar and a confining geometry contributed to the variations in the critical heat flux. The reason boiling heat transfer in a confined geometry reduced the overall

effects of any natural convection was that the resultant bubbles could not disperse as easily.

The second part of the analyses was from a dynamical systems point of view in which the time evolution of the heat transfer system was of primary concern. Here steady state measurements yielded data which were not so steady afterall, were analyzed. This work consisted of examining the evolution (in time) of the fluctuating system variables  $\dot{Q}$  and  $T$  to see whether any insight or predictive information could be gained. Some aspects of this analysis worked better than others, but with experimental and analytical refinements, improvement seems possible. For example, by observing that the "circulation" of the heat flux and temperature reaches a peak as the transition to film boiling was approached, a possible precursor to film boiling was discovered. The other analyses such as the Fourier spectrum or correlation dimension calculations gave inconclusive results. On the other hand, this research produced some interesting and unanswered physics questions concerning the nature of nucleation. "Can single nucleation sites behave in a chaotic matter? " and " Do aggregates of these sites behave in some sort of collective manner which can be described by simple, low dimensional dynamics? "

Overall, these results have added significant new data to the heat transfer literature, and indicate that previously neglected questions in heat transfer are

important after all. This study also generated some interesting insights and novel analyses for a very traditional subject. Hopefully, this course of inquiry will encourage new research or a continuation of this work.

## REFERENCES

1. P. Komarek, The implications of higher critical temperature superconductive materials, in *Proceedings of the twelfth Int. Cryogenic Engineering Conference* Butterworth, Guildford, U.K. (1988) p. 64.
2. R.K. Kirschman, Cold electronics: an overview, Cryogenics (25) 115 (1985).
3. G.M. Chrysler, and R.C. Chu, cooling of high power density electronic chips, in: *Advances in Cryogenic Engineering*, vol. 35, Plenum Press, New York (1990).
4. W. Frost (ed.), *Heat Transfer at Low Temperatures*, Plenum Press (1975).
5. Y.S. Touloukian et al, *Thermal Diffusivity*, Vol. 10 of *Thermophysical Properties of Matter*. Plenum Press, New York (1973).
6. D.N. Sinha et al, Premature transition to stable film boiling initiated by power transients in liquid nitrogen, Cryogenics 19(4):225 (1979).
7. Eric W. Roth, Erik Bodegom, L.C. Brodie, and J.S. Semura, in: *Advances in Cryogenic Engineering*, Vol. 35A, Plenum Press, New York (1989), p. 447.
8. P.J. Giarratano, Transient boiling heat transfer from two different heat sources: small diameter wire and thin film flat surface on a quartz substrate, Int. J. Heat Mass Transfer 27(8):1311 (1984).
9. A.C. Rose-Innes, and E.H. Roderick, *Introduction to Superconductivity*, 2nd ed. Pergamon Press (1978).
10. P.G. Koskey and D.N. Lyon, Pool boiling heat transfer to cryogenic liquids, AIChE Journal; May, 1968 p. 372.
11. J.R. Holman, *Heat transfer*, 5th ed. McGraw-Hill, New York (1981).
12. M. Blander and J.L. Katz, Bubble Nucleation in Liquids, AIChE Journal; September, 1975 p. 833.

13. W.M. Rohsenow (ed.), *Handbook of Heat Transfer* 3rd ed. McGraw-Hill, New York (1973).
14. V.P. Skripov, *Metastable liquids*, Wiley, New York, (1974).
15. D.N. Sinha, L.C. Brodie, and J.S. Semura, Liquid-to-Vapor Homogeneous Nucleation in Liquid Nitrogen, Phys. Rev. B36(7):4082 (1987).
16. P.G. Knibbe, The End-Effect Error in the Determination of Thermal Conductivity Using a Hot Wire Apparatus, Int. J. Heat Mass Transfer. Vol 29, No. 3, p.463 (1986).
17. B. HaOkansson, P. Andersson, and G. Bäckström, Improved Hot-Wire Procedure for Thermophysical Measurements under Pressure, Rev. Sc. Instrum. 59:2269 (1988).
18. L.A. Hall, Survey of Electrical Resistivity Measurements on 16 Pure Metals in the Temperature Range 0 to 273 K. NBS Tech. Note 365-1. National Bureau of Standards, Boulder, Colorado (1968).
19. H.S. Carslaw, J.C. Jaeger, *Conduction of Heat Solids* 2nd ed., Oxford University, London (1959) p.344.
20. O. Tsukamoto, T. Uyemura, and T. Uyemura, Observation of bubble formation mechanism of liquid nitrogen subjected to transient heating, in: *Advances in Cryogenic Engineering*, Vol. 25, Plenum Press, New York (1980), p.476.
21. J.S. Trefil, *Introduction to the Physics of Fluids and Solids*, Pergamon Press, New York (1975).
22. Roderick Jensen, Classical chaos, American Scientist vol. 75 March-April (1987) p. 168.
23. E.A. Jackson, *Perspectives of Nonlinear Dynamics*, Vol.1, Cambridge University Press (1989).
24. E.N. Lorenz, Deterministic nonperiodic flow, J. Atmos.Sci vol. 20 p.130 (1963).
25. H.L. Swinney and J.P.Gollub, The transition to turbulence, Physics Today 31(8),41 (1978).
26. P. Bergé, Y. Pomeau, and C Vidal, *Order within Chaos*, John Wiley and Sons (1984).
27. L. E. Reichel, *A modern course in statistical physics*, University of Texas Press, Austin (1980).

28. Peter Grassberger and Itamar Procaccia, Measuring the strangeness of strange attractors, Physica 9D (1983) p.189.
29. B.B. Mandelbrot, *The fractal geometry of nature*, W.H.Freeman (1983).
30. N. Gershenfeld, in: *Directions in Chaos*, vol. 2, ed. B.I. Hao, World Scientific Press, (1988)
31. M. Hénon, Numerical study of quadratic area-preserving mappings, Quart. of Appl. Math 27, p. 291 (1969).
32. F. Takens, Detecting strange attractors in turbulence, in: *Dynamical Systems and Turbulence, Warwick 1980* Lecture Notes in Mathematics 898, ed. D.A. Rand and L.S. Young, Springer-Verlag.
33. N.H. Packard et al, Geometry from a time series, Phys. Rev. Letters 45, p. 712 (1980).
34. H. Whitney, Differentiable manifolds, Ann. Math. 37, p.645 (1936).
35. M. Casdagli, State space reconstruction in the presence of noise, Physica D 51 (1991) p. 52.
36. A.M. Fraser and H.L. Swinney, Independent coordinates for strange attractors from mutual information Phys. Rev. A vol. 33, (1986) p. 1134.
37. W. Liebert and H.G. Schuster, Proper choice of the time delay for the analysis of chaotic time series, Phys Letters A, vol. 142 number 2,3 (1989) p. 107.
38. G.A. Bennetin, On the reliability of numerical studies of stochasticity, *Nuovo Cimento* 44B (1978) p. 183.
39. A. Ben-Mizrachi and I. Procaccia, Characterization of experimental (noisy) strange attractors, Phys. Rev. A vol. 29, (1984) p. 975.
40. L. Smith, Phys Letters A, vol. 133 (1988) p. 283.
41. J.P. Eckmann and D. Ruelle, Fundamental limitations for estimating dimensions and Lyapunov exponents in dynamical systems, Physica D 56 (1992) p. 185.
42. H.G. Schuster, *Deterministic chaos: an introduction*, 2nd ed., VCH, Cambridge (1988).

43. N.A. Gershenfeld, Dimension measurement on high-dimensional systems Physica D 55 (1992) p. 135.
44. R. Badi et al, Dimension increase in filtered chaotic signals Phys. Rev. Letters 60, p. 979 (1988).
45. R. Shaw, *The dripping faucet as a model chaotic system*, Aerial Press, Santa Cruz, CA (1984) p. 368.
46. R.F. Cahalan et al, Chaotic Rhythms of a dripping faucet, Computers in Physics, Jul/Aug (1990).

## APPENDIX

### BUBBLE DROP EXPERIMENT

In view of the problems mentioned in Chapter VIII, an alternative and simplified experiment was to observe what occurs at just one bubble site. However, this is not really the same problem as discussed previously because the system has been simplified too much. Having one isolated bubble site means there is not any interaction with other bubble sites. The most that could be learned concerns the dynamics of a single nucleation site. The process of pool boiling developing into film boiling is a collective phenomenon, and this collective process was the desired observable. Nonetheless, characterizing the fundamental component of the system, the nucleation site, is an important step to understanding the boiling process as a whole. Therefore an experiment was devised in an analogous fashion to Shaw's often studied chaotic water drop experiment [45,46]. In Shaw's experiment the time between drops originating from a dripping water faucet was observed. At low average drop rates the drops detach periodically, but with increasing drop rates there was more than one period, and finally the drop rates appear to vary chaotically from drop to drop.

In the single bubble site experiment, bubbles from one

nucleation site were created and observed, to obtain quantitative values for bubble velocity and departure rates. The analysis is similar to Shaw's in that the various periodicities of the bubble departure rates were the main observable.

Because of the limitations of the heater/thermometer previously discussed, a new apparatus was designed that gives information other than temperature and heat flux. The variables that could then be observed were the bubble diameter, velocity and departure rate. It was not possible to measure the temperature, and the heat flux was only known on a relative scale. The single bubble generator was fabricated as follows (see Figure 20). A cylinder 3.5 cm in diameter and 2 cm long was constructed out of an insulating material (TEFLON). Towards the top inside portion of the cylinder was placed a small diameter (0.4 cm) metal rod wrapped with thin gauge wire in which current was passed to provide Joule heating. An additional vertical hole (0.6 mm dia.) was made through the top of a cover plate down to the heater. This cover plate could be interchanged so that different size cavities could be tested. This cavity was the artificial nucleation site and produces bubbles nominally 1.2 mm in diameter when heat was dissipated in the wire. Note this size was considerably larger than the 0.2 mm bubbles seen originating from the platinum wire and corresponds to a vapor volume over 200 times larger.

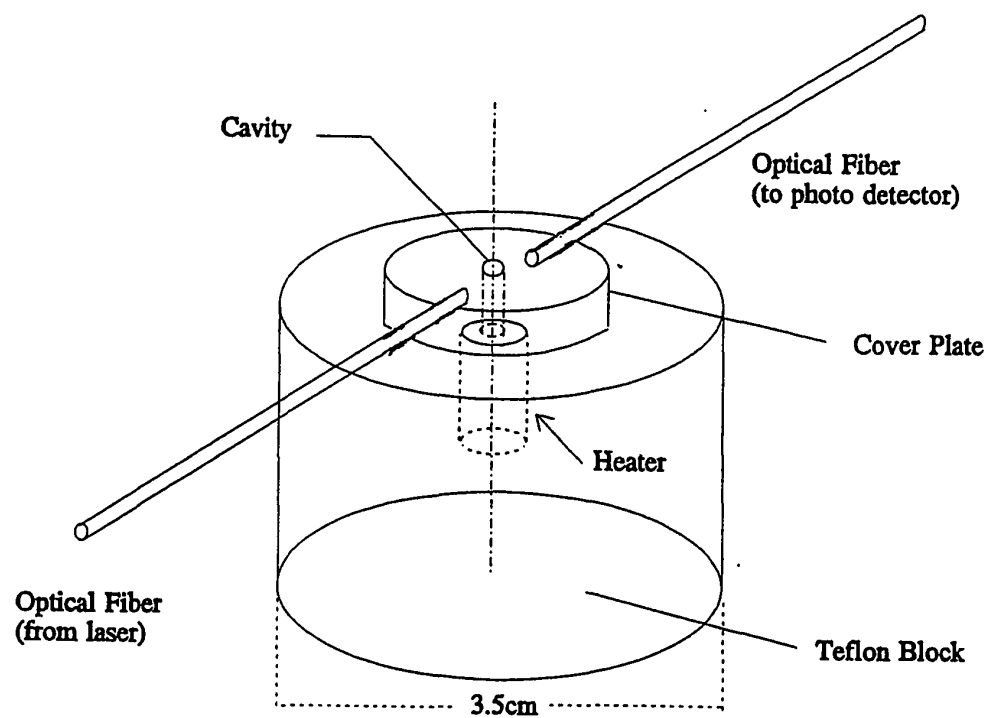


Figure 20. Schematic of bubble generator.

However, this was intentional because of the limited sensitivity of the bubble detection apparatus.

Bubble detection was achieved by optical measurements. Light from a helium-neon laser was routed through a plastic optical fiber (1.4 mm dia. core) into the dewar and aligned adjacent to the nucleation site. Directly opposite this was another fiber which receives the laser light and transmits it to a photodiode/amplifier assembly outside the dewar. When the bubble passes between the fibers it scatters the incoming laser light, thus reducing the light detected by the photodiode. The scattering effect was not large and was the reason that very small bubbles, though visible to the eye, could not be detected by the electronics. The photodiode and amplifier assembly have a response time shorter than 10  $\mu s$ , more than adequate for observing the bubbles which had departure times greater than 10 ms. After low pass filtering the amplified photodiode output, the analog voltage signal was digitized at a rate of 10,000 per second and stored in the computer. The bubble diameter and velocity were measured from recordings made with a home video camera; however, resolution was limited due to performance limitations of the camera. Some of the conclusions reached are as follows. The bubble reached terminal velocity of 100 cm/sec 20 ms after release from the artificial nucleation site.

The primary analysis consisted of calculating the

elapsed time between bubble departures. A computer program was written such that the positions (in the time series) of the local minima in the photodiode signal level was recorded. These minima corresponded to bubbles passing through the detector and blocking the light received by the photodiode. These bubble departure times were then plotted vs. the bubble number to see whether any patterns emerge. The sequence of graphs in Figure 21 are from low heater currents to high ones. As can be seen from the top plot there is a characteristic time between bubbles of 310 ms. There was also a second characteristic time of 760 ms that occurs after the passage of approximately 20 bubbles. Similar interesting patterns can be seen from the other two plots. Upon reflection, this was an unexpected result. Typically, one would expect some mean bubble departure time that had a normally distributed uncertainty. In fact, these patterns are reminiscent of those seen in Shaw's water drop experiment before chaos had set in. However, the results are problematic in that the reproducibility is poor. Even though many of the data sets show two or more characteristic times in a very regular fashion, if one attempts to repeat a run under the exact experimental conditions, different results could be obtained. For example, the apparatus could be removed from the dewar, warmed to room temperature, and then reinserted into the LN<sub>2</sub>. The new data set could yield different results than the previous set. Also, the device

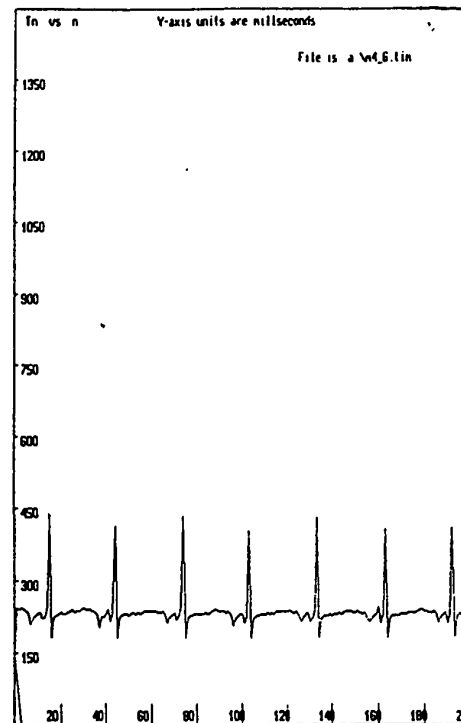
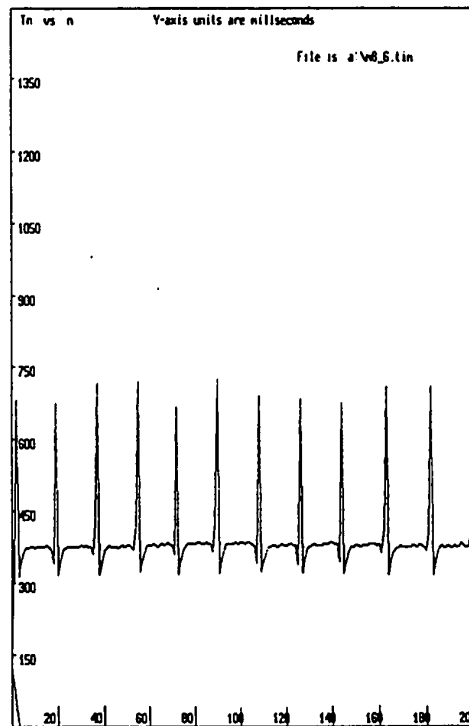


**Figure 21.** Time Between Bubble Departures vs. Bubble Number.

could be left bubbling over night at a constant heater current, but the next morning the characteristic times change or disappear altogether. No conclusive reason for this behavior has been found. Possible reasons are that the cavity and heater interface did not make a reliable and unchanging cavity size. Also, ice crystals might be forming in or around the cavity. This could have an effect on the surface tension affixing the bubble to the cavity opening or block the cavity entrance. So while it appears that something interesting was going on here, possibly akin to the Faucet Drop Experiment, there are too many experimental uncertainties to be worked out presently. However, it appears that this could be a fruitful and interesting project on its own accord.